Air Force Institute of Technology

AFIT Scholar

12-1995

A Comparison of Methods for Estimating RMS Error: A `Brute Force" Approach Versus a Mathematically-Elegant Approach, as Applied to the Calculation of a Specific Retrieval Error for a Limb-Scanning Microwave Radiometer-Spectrometer

Larry L. Johnson

A Comparison of Methods for Estimating RMS error:
A "Brute Force" Approach Versus a Mathematically-
Elegant Approach, as Applied to the Calculation of a
Specific Retrieval Error for a Limb-Scanning Microwave
Radiometer-Spectrometer

THESIS

Larry L. Johnson, Captain, USAF

AFIT/GAP/ENP/95D-10

DEPARTMENT OF THE AIR FORCE

AIR UNIVERSITY

AIR FORCE INSTITUTE OF TECHNOLOGY

DTIC QUALITY INSPECTED 3

Wright-Patterson Air Force Base, Ohio

Accesion For		
NTIS CRA&I		☒
DTIC TAB		☐
Unannounced		☐
Justification		
By		
Distribution /		
Availability Codes		
Dist	Avail and / or Special	
A-1		

A Comparison of Methods for Estimating RMS error:
A "Brute Force" Approach Versus a Mathematically-
Elegant Approach, as Applied to the Calculation of a
Specific Retrieval Error for a Limb-Scanning Microwave
Radiometer-Spectrometer

THESIS

Larry L. Johnson, Captain, USAF

AFIT/GAP/ENP/95D-10

DTIC QUALITY INSPECTED 3

A Comparison of Methods for Estimating RMS Error:

A "Brute Force" Approach Versus a Mathematically-Elegant Approach, as Applied to

the Calculation of a Specific Retrieval Error for a Limb-Scanning Microwave

Radiometer-Spectrometer

Larry L. Johnson, B.A., B.S.

Captain, USAF

Approved:

27 Nov 95

Derrill T. Goldizen, Captain, USAF
Chairman, Advisory Committee

28 Nov 95

David L. Coulliette, Major, USAF
Member, Advisory Committee

27 Nov 95

David E. Weeks
Member, Advisory Committee
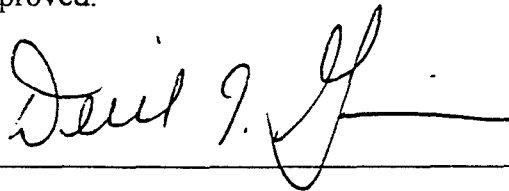
A Comparison of Methods for Estimating RMS Error:

A "Brute Force" Approach Versus a Mathematically-Elegant Approach, as Applied to

the Calculation of a Specific Retrieval Error for a Limb-Scanning Microwave

Radiometer-Spectrometer

THESIS

Presented to the Faculty of the School of Engineering

Air Education and Training Command

In Partial Fulfillment of the Requirements for the Degree of

Masters of Science in Information Resource Management

Larry L. Johnson, B.A., B.S.

Captain, USAF

December 1995

Acknowledgments

I would like to thank Major David L. Coulliette and Dr. David E. Weeks whose contributions as members of my advisory committee were indispensable. I would especially like to thank Captain Derrill T. Goldizen, my thesis advisor. His guidance and patience through the entire thesis process made this paper possible.

I could not have completed this work without the encouragement and support of my wife Stacey Mason-Johnson. Even when she was busy with her own work during her first year in law school, she took the time to listen to my complaints when things weren't working correctly, and she even did the first complete edit of my work. Even when it seemed the computer was more important than our marriage, she encouraged me to continue.

TABLE OF CONTENTS

CHAPTER 5: Experimental Results

CHAPTER 6: Conclusions

Appendix A

Appendix B

Appendix C

Appendix D

TABLE OF FIGURES

A Comparison of Methods for Estimating RMS Error:
A "Brute Force" Approach Versus a Mathematically-Elegant
Approach, as Applied to the Calculation of a Specific Retrieval
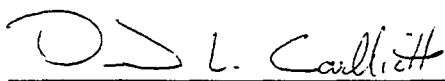**Error for a Limb-Scanning Microwave Radiometer-Spectrometer**

Capt. Larry L. Johnson
AFIT/GAP/ENP/95D-10
Advisors: Major David L. Coulliette (ENC), Capt. Derrill T. Goldizen (ENP),
and Dr. David E. Weeks (ENP)
Sponsor: Dr. Richard Bevilacqua
Space Sciences Division
Naval Research Laboratory

The Millimeter-wave Atmospheric Sounder (MAS) is a high resolution limb-scanning microwave radiometer-spectrometer which has been flown aboard the Space Shuttle. The instrument was designed to sense the microwave emission from several upper atmospheric constituents, including water vapor and ozone.

The resonant frequencies of water vapor and ozone are extremely close (183 and 184 GHz, respectively), so that the high-frequency wing of the water vapor spectrum overlaps the low frequency wing of the ozone spectrum. Consequently, the measured ozone spectrum incorporates a slight water vapor contribution; therefore, the retrieved ozone profile is dependent on the true water vapor profile.

The MAS operational retrieval algorithm uses the ozone measurement spectrum to retrieve the height dependent vertical ozone concentration profile, but requires a water vapor profile in order to remove the influence of the water vapor spectrum from the ozone spectrum. Currently, the MAS Science Team provides the retrieved water vapor profile as the input to the ozone retrieval algorithm. Our simulation study investigates if this technique results in a smaller error than one in which a single, fixed climatological-mean water vapor profile is employed for all the ozone retrievals.

In answering this question, two error analysis approaches are compared: a simulation study involving 100 synthetic ozone spectra for which an ensemble RMS error between true and retrieved ozone values is calculated, versus a single, elegant, but mathematically-complicated calculation of the associated error covariance matrix as suggested by C. D. Rodgers [1990].

CHAPTER 1

Introduction

1.1 Experimental Background

The Millimeter-wave Atmospheric Sounder (MAS) is a limb-scanning, passive-microwave radiometer-spectrometer which was first flown aboard the Space Shuttle in March of 1992. The instrument flew annually from 1992 through 1994 on seven to ten day missions, but due to reduction in funding, the experiment was discontinued in 1995. The MAS provides high-resolution pressure broadened emission spectra from rotational transitions of ozone, water vapor, chlorine monoxide, and molecular oxygen between the altitudes of 17-80 kilometers. Limb-scanning geometry is used to recover high resolution vertical profiles of atmospheric constituents because the measured emission comes from a very narrow region around the tangent point (Fig 1.1).

The MAS constituent spectra are measured from within the same atmospheric volume. The resonant lines of ozone and water vapor are so close that the upper sideband of the water vapor spectrum contaminates the lower sideband of ozone spectrum. The MAS inverse model uses an *a priori* (assumed) water vapor profile to account for this contamination when retrieving an ozone profile from the measurement.

A measured spectrum is a spectrum of the atmospheric constituent as measured by the MAS. Each water vapor or ozone measured spectrum data file contains 21 measured spectra of the constituent in question at altitudes between 20 and 80 km in 3 km intervals. 50 brightness temperature measurements are made, each at a different

Tangent Point

Cold Space
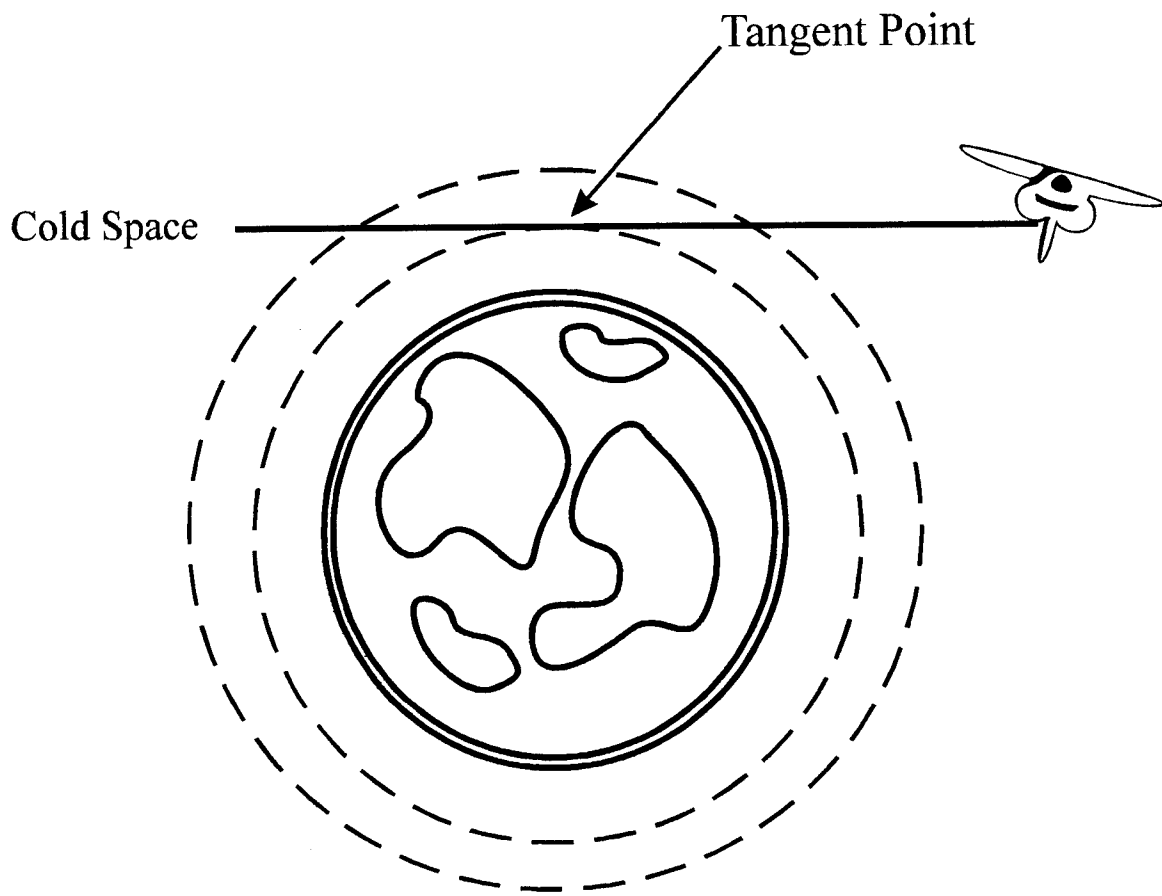
Fig 1.1 Limb Scanning Geometry of MAS System

2

frequency, at each altitude. The result is a brightness temperature spectrum for an individual species at each of the above mentioned altitudes.

The retrieval vector is the vector which results when a measured spectrum is ran through the MAS inverse model (see section appendix A). Each retrieval vector contains 22 volume mixing ratios, each at a different altitude, which together compose a vertical profile of the constituent in question. Also in the a retrieval vector are values for the angular offset and the sideband ratio.

1.2 Purpose of the Research

Ozone in the upper atmosphere helps reduce the amount of harmful ultraviolet radiation reaching the Earth's surface. This paper investigates the error contribution of an *a priori* water vapor profile on the retrieval of ozone from radiometric measurements in the upper atmosphere. The *a priori* water vapor profile is used to remove the influence of a spectrally adjacent water vapor resonant feature (183.31 GHz) on the measured ozone spectrum centered on 184.37 GHz (the companion gas problem). The MAS science team currently uses the associated retrieved water vapor profile (retrieved from water vapor emission within the same atmospheric volume as that of the corresponding ozone spectrum) as the *a priori* profile when running an ozone spectrum through an inverse model to recover a vertical ozone profile. One question is whether this retrieval process results in less error than one that uses a climatological mean water vapor profile (a "fixed" *a priori*) for all ozone retrievals. Also investigated is how

3

accurately the MAS inverse model retrieves two instrument parameters (angular offset and sideband ratio) from the data.

In the investigation, two error analysis methods are compared. The first is a "brute force" method of calculating the root mean square error using all ozone retrievals. The second is an elegant but more complicated method described by C. D. Rodgers in 1990. This paper will compare the results of these two error methods in the investigation of the companion gas retrieval problem (see section 2.3) in hopes of validating Rodgers' technique.

1.3 Thesis Organization

The paper is divided into 6 chapters, each describing a certain aspect of the experiment. Chapter 2 defines the problems investigated in the simulation experiment and clarifies how these problems can affect results. Chapter 3 presents the general mathematical theories used in the error analyses. Chapter 4 describes the experimental procedures used to investigate the problems described in chapter 2. Chapter 5 discusses results obtained from the experiment. Chapter 6 states the conclusions drawn from these results.

CHAPTER 2

Definition of Retrieval Problems

2.1 Introduction

This chapter describes in detail the angular offset and sideband ratio retrieved parameters and how they can affect **all** retrievals. The companion gas problem affects only the retrieval of water vapor and ozone. The impact these parameters might have on the retrieved profile is also clarified.

2.2 Angular Offset Problem

A remote sensing feedhorn senses radiation which is focused on it by an antenna. The MAS was designed so that the oxygen feedhorn is precisely aligned with the focal plane of the antenna. The ozone/water vapor and chlorine monoxide feedhorns are aligned slightly off the focal plane because they share the radiation field emerging from the same beam-splitter [Goldizen, 1995]. The slightest mismeasurement of this offset can significantly alter the retrieved altitudes. The following is an example which demonstrates the affect of the offset on the retrieved altitudes.

Assume the Space Shuttle is at 60 degrees north latitude at a height of 300 kilometers. The angle between the local vertical at the tangent point and the incident beam will be 90 degrees (since the tangent to a circle is always normal to the radius of the circle passing through the tangent point). If we assume the feedhorn measuring the

constituent is in alignment with the focal plane of the antenna then the tangent height can be found using the following relationship:

$$H_T = (Z + R_e) \sin(\alpha) - R_e \qquad\qquad [2.1]$$

Here Z is the orbital altitude of the platform, R_e is the radius of the earth (6370 kilometers), H_T is the tangent height, and α is the "look angle" (the angle between Space Shuttle vertical and the incident beam). The look angle varies between 73.25 degrees (for a tangent height of 17 kilometers) and 75.24 degrees (for a tangent height of 80 kilometers). For this example assume the look angle to be 74.17 degrees which results in a tangent height of 47 kilometers (Fig 2.1).

From the above example, if we now allow the feedhorn to be off alignment by 0.1 degrees upward, the original tangent height H_T is increased by the amount h_T (Fig 2.2). To determine the value of h_T, the distance from the tangent point to the orbiting platform must be found. This distance is computed using the Pythagorean theorem since we already know H_T.

$$D^2 = (R_e + Z)^2 - (R_e + H_T)^2 \qquad\qquad [2.2]$$

Here D is the distance form the tangent point to the orbiting platform (in this case the Space Shuttle), R_e is the radius of the earth, Z is the altitude of the orbiting platform, and H_T is the tangent height defined by equation 2.1. Once the value for D has been determined, h_T can be found using the tangent function.

$$h_T = D \times \tan(0.1) \qquad\qquad [2.3]$$
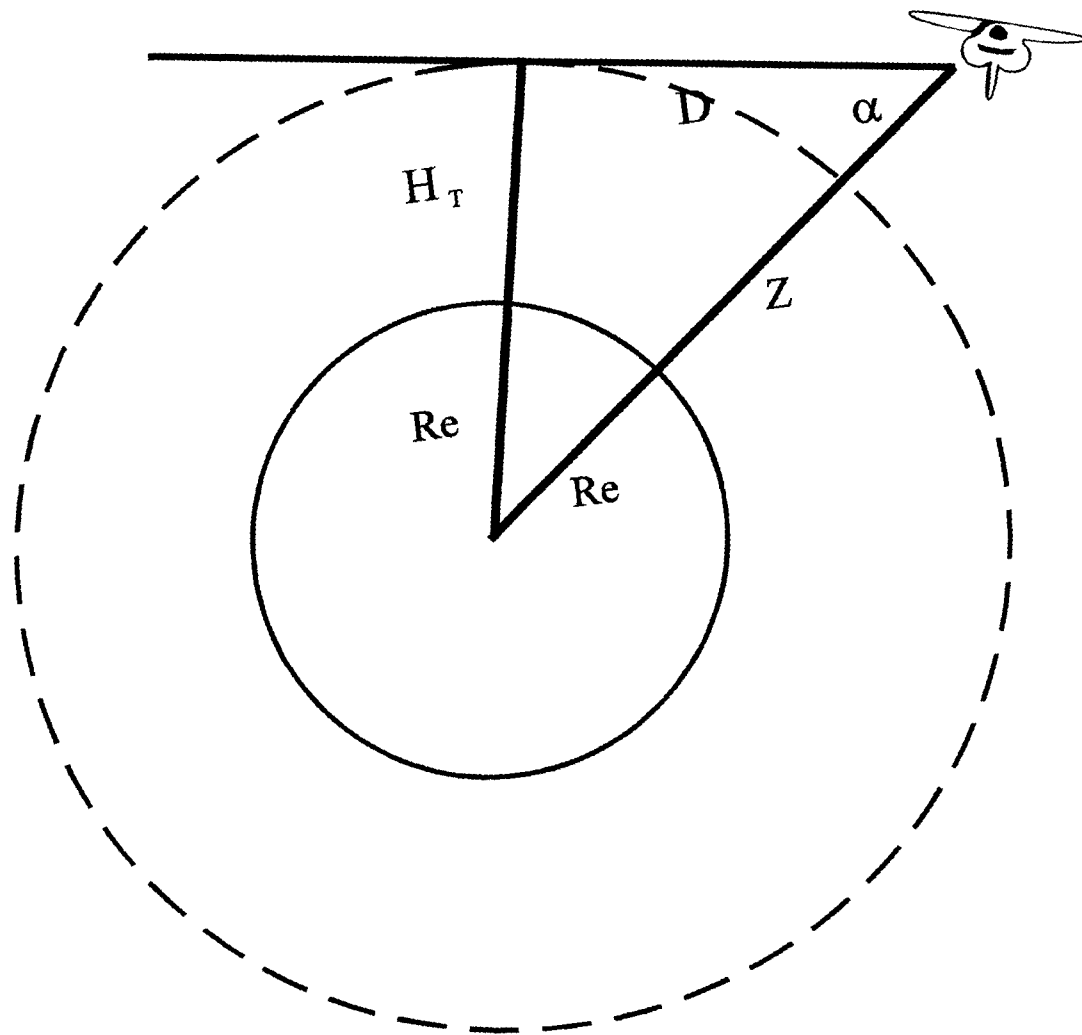
Fig 2.1 Geometry of Limb-Scanner with Aligned Feedhorn
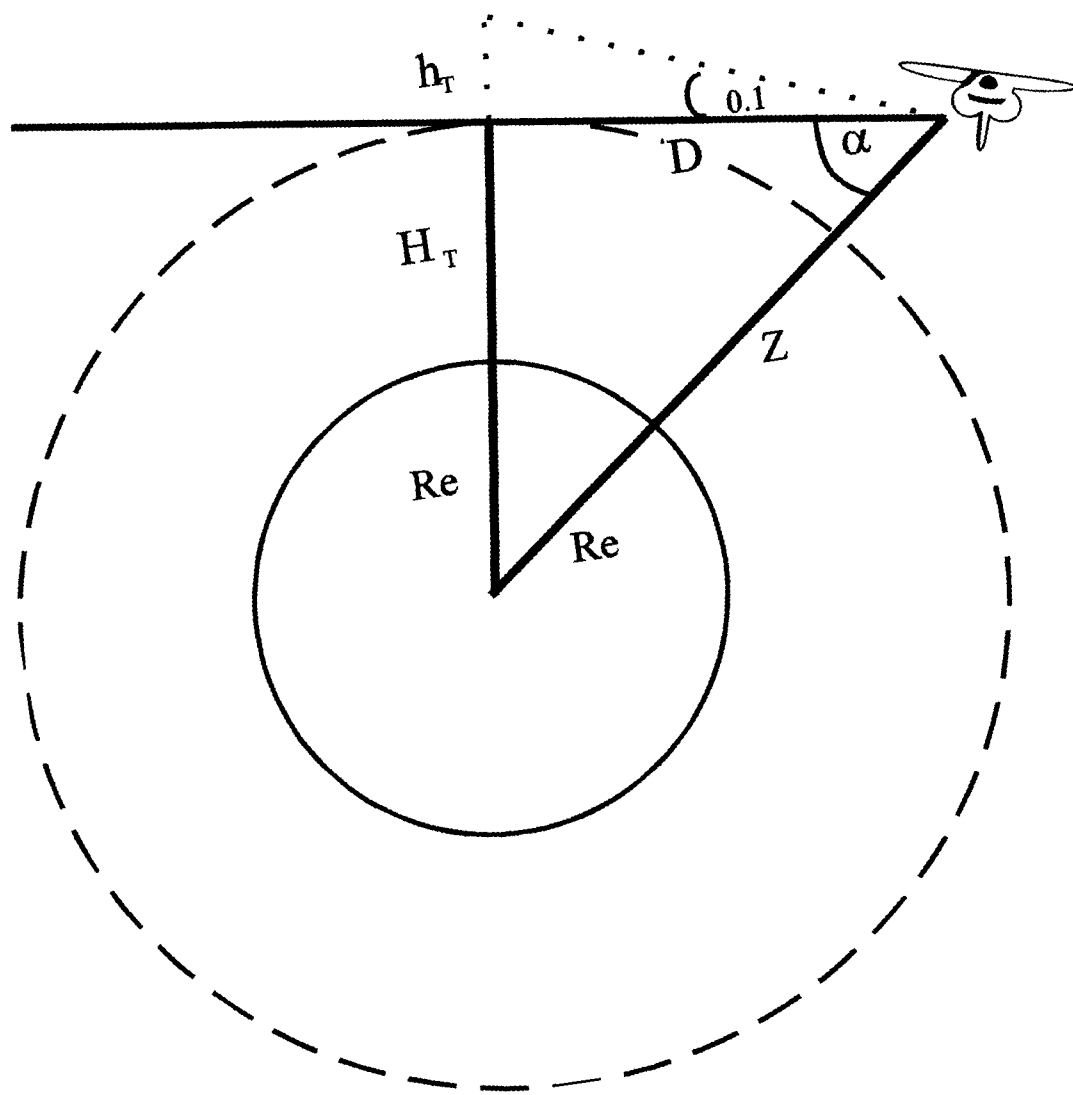
Fig 2.2 Geometry of Limb-Scanner with Angular Offset

The values computed using the above assumptions show the change in tangent height to be 3.18 kilometers. The measured spectrum varies greatly over one kilometer so a variation in the measured altitude on the order of 3 kilometers will have a profound affect on the retrieved profile.

The angular offset for the ozone/water vapor feedhorn was determined to be approximately -0.11 degrees during the lunar calibration experiment of ATLAS-2. The MAS science team was skeptical of the method used to determine this value and the uncertainty in the Shuttle's roll axis position did not allow the MAS to use GNC (guidance and navigation computer) data to accurately determine the tangent height. Therefore the angular offset is a retrieved parameter.

2.3 Companion Gas Problem

The measured water vapor and ozone resonant frequencies are close to one another (183.31 GHz and 184.38 GHz respectively). Because of this proximity, there is some contamination of the ozone spectrum by the upper sideband of the water vapor spectrum (Fig 2.3). This contamination must be accounted for somewhere in the inverse model or the retrieved ozone profile will not be an accurate representation of the true ozone profile. The contamination of the water vapor spectra from the upper sideband of the ozone spectra is insignificant because the line strength of water vapor is ten times greater than that of ozone. Any contamination of a water vapor spectrum by an ozone spectrum is minimal and therefore ignored.

The MAS inverse model uses an optimal estimation routine to retrieve a profile from a measured spectrum. To retrieve an ozone profile from the measured ozone
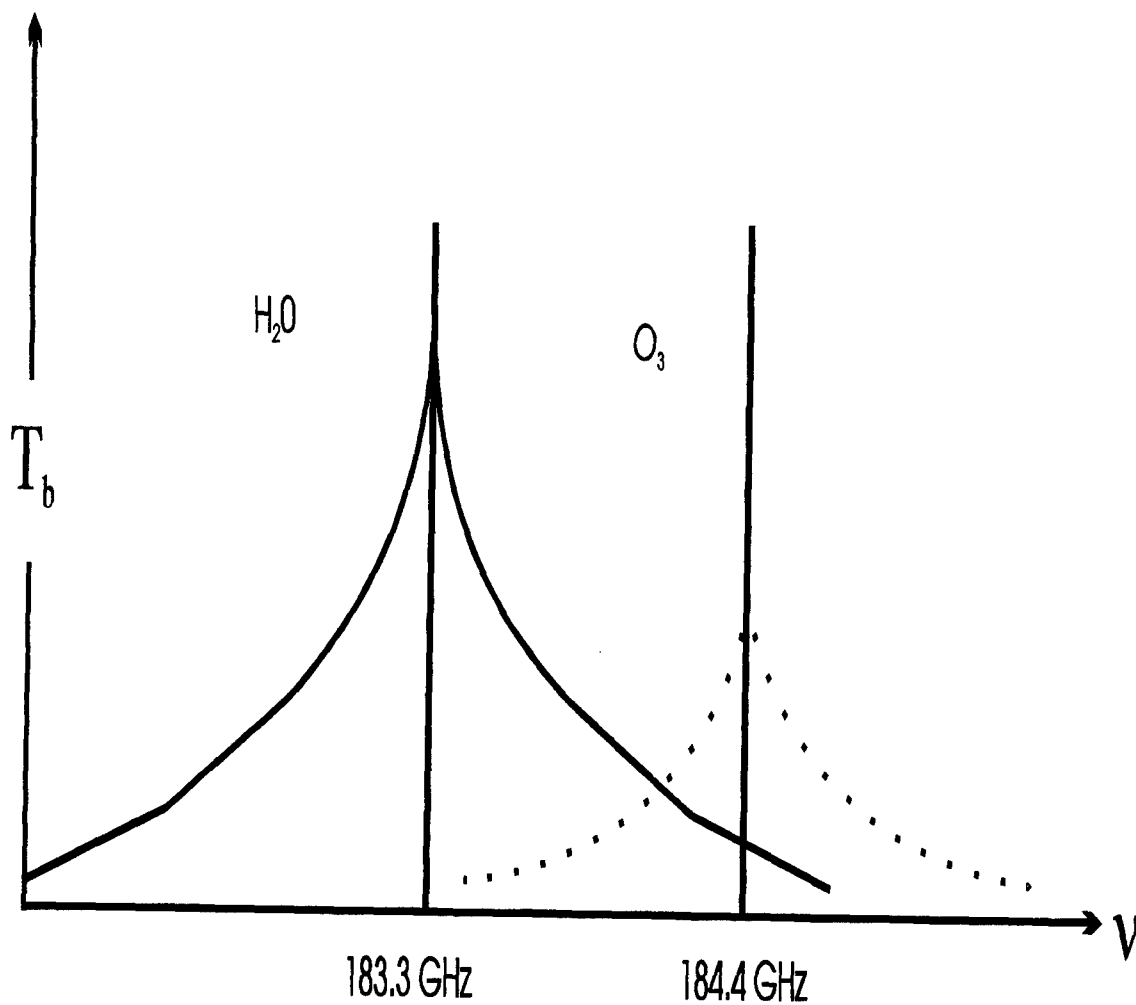
Fig 2.3 Brightness Temperature (T_b) Spectrum for Ozone and Water Vapor
(Not to Scale)

spectrum, this routine requires an *a priori* estimate of the water vapor profile. Currently

the MAS science team uses as the water vapor *a priori* the water vapor profile retrieved

from a measured water vapor spectrum received at the same time as the desired ozone

spectrum.

2.4 Sideband Ratio Problem

The MAS instrument incorporates a mixer-local oscillator for the purpose of

converting the millimeter-wave signal (183-184 GHz) to a lower frequency (1-6 GHz)

which is more easily processed by the follow-on circuitry. Because the mixer used is a

double sideband mixer, the sideband below the local oscillator frequency (lower

sideband or image band) is "folded" into the sideband above the local oscillator

frequency (upper sideband or signal band). This is shown in (Fig 2.4). The resonant

feature, which is what is desired to be retrieved, is located in the upper sideband. This

result, the lower sideband being "folded" into the upper sideband, will contaminate the

measured spectral image. The contamination may be removed if the sideband ratio is

known.

The sideband ratio relates the total signal measured by the radiometer to

the desired target signal and its image contribution :

$$\mathbf{T_M}(v) = \mathbf{R} \times \mathbf{T_a}(v) + (1-\mathbf{R}) \times \mathbf{T_I}(v) \qquad [2.4]$$

Where $\mathbf{T_I}$ is the image band contribution, $\mathbf{T_M}$ is the signal measured by the radiometer,

$\mathbf{T_a}$ is the desired target signal and v is the frequency. From this equation the image band

11
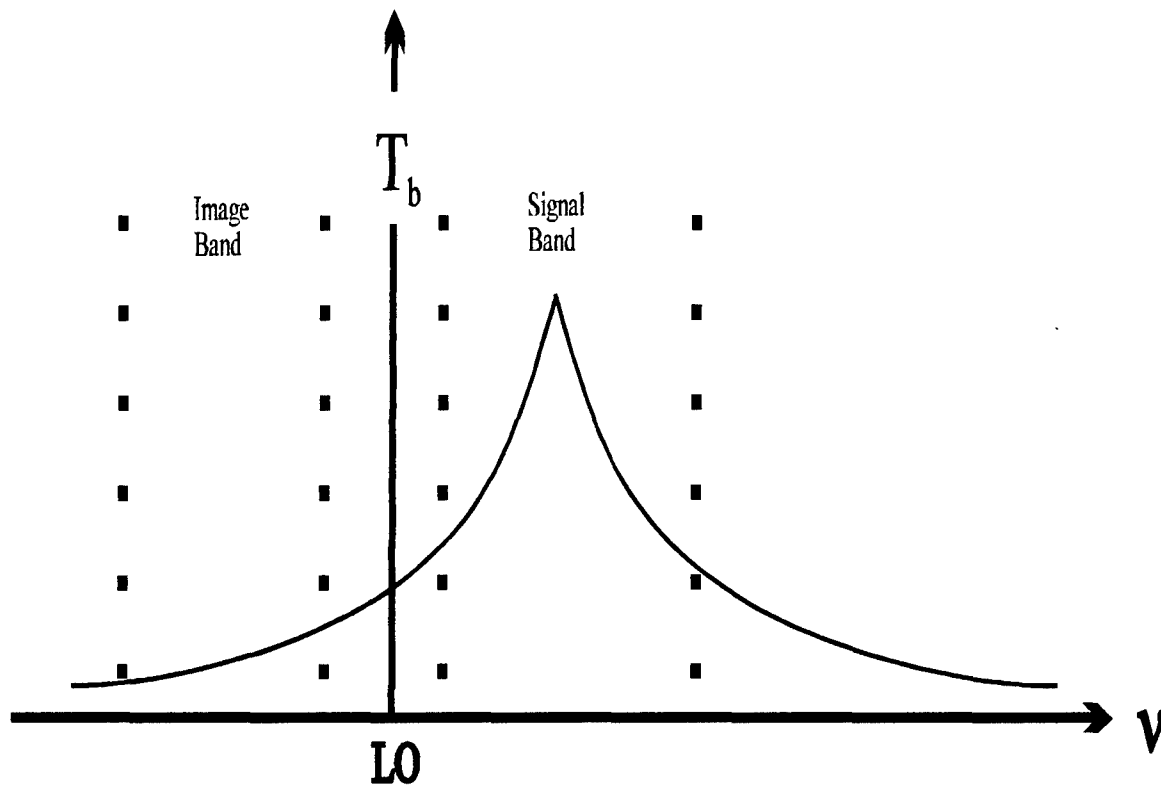
Fig 2.4 Brightness Temperature (T_b) Spectrum. The Image Band is "Folded" into the Signal Band Around the Local Oscillator (LO) Contaminating the Retrieval. This can be Compensated for if the Side Band Ratio is Known.

($\mathbf{T_I}$) influence on the desired signal can be removed. The sideband ratio value is usually determined through laboratory calibration. This was not possible for the MAS system due to the tight construction and testing schedule imposed by NASA. The sideband ratio is a retrieved parameter in the MAS data reduction scheme [Goldizen, 1995].

CHAPTER 3

Mathematics of Error Analysis

3.1 Introduction

This chapter will explain the general mathematical approaches behind the two error analysis methods used. The application of these approaches to the retrieval problem is described in sections 4.5 and 4.6.

3.2 Root Mean Square Error

The root mean square error calculation is a well known and frequently used method of error analysis. It accurately depicts the magnitude of deviations of and estimated (measured or calculated) value from the actual value sought. The general equation for root mean square error (RMSE) is:

$$RMSE = \sqrt{\frac{(\sum_{i=1}^{n}(a_i - b_i)^2)}{n}} \qquad [3.1]$$

where **n** is the total number of estimated values to be evaluated, **a** is the calculated value, and **b** is the known "true" value.

3.3 Rodgers' Error Analysis

Rodgers' error analysis is a more complicated method. Here we describe the mathematical details as they apply to the MAS error analysis .

The measured spectrum can be expressed as a function of the true profile and a vector of parameters which might be part of the true profile but are not retrieved from the measurement spectrum. These parameters might be an assumed profile or some values related to the forward model and instrument:

$$Y = F(X, b)$$ [3.2]

where Y is the measured spectrum vector, X is the true profile vector, b is the vector of non-retrieved parameters, and F is the forward model.

Generally Y is measured. An inverse model can be used, given Y and the associated measurement error, to find an estimate of X (the retrieved profile).

$$X_R = I(F(x, b), \varepsilon_y) = I(Y, \varepsilon_y)$$ [3.3]

Here X_R is the retrieved profile vector, I is the inverse model, and ε_y is the measurement error vector.

The sensitivity of the retrieved profile to non-retrieved parameters is expressed in the following equation:

$$[D_b]_{(i,j)} = \frac{\partial X_R}{\partial b} = \left[\frac{\partial (X_R)_i}{\partial b_j} \right]$$ [3.4]

where the jth column of D_b describes how the retrieval (X_R) responds to a perturbation in the jth component of the vector b. $(X_R)_i$ is the ith component of the retrieved ozone profile vector, or the retrieved ozone concentration at the ith atmospheric level.

In Rodgers' error analysis, a covariance matrix is required. The entry in the first row of the first column is the variance of the first component of the first retrieval with the first component of all retrievals. The second element in the first column is the

15

covariance of the second level of the first retrieval with the first level of all retrievals. The result is a square matrix with variance values as the diagonals and the off diagonals equal to the covariance of the retrievals. The square root of the variance is equivalent to the RMS error. This matrix can be generated using the following equation:

$$[S_b]_{(i,j)} = \overline{(X_R)_i \times (X_R)_j} - \overline{(X_R)_i} \times \overline{(X_R)_j} \qquad [3.5]$$

where i is the row and j is the column of the matrix S. $(X_R)_i$ is the ith row of the retrieved parameter, and $(X_R)_j$ is the jth row of the retrieved matrix. The overbar represents a mean value calculation.

The above matrices are then used to compute the total error matrix. The square root of the diagonals of this matrix are the RMSE values of the retrieval at different altitudes (component) of the retrieved profile vector.

$$S_T = D_b S_b D_b^T \qquad [3.6]$$

Here S_T is the total error matrix with D_b and S_b defined above [Rodgers, 1990].

CHAPTER 4

Numerical Experimental Procedures

4.1 Introduction

This chapter describes the numerical experiment used to investigate the problems described in chapter 2. Included is the description of how the true profiles were developed and how they were used later in the experiment.

4.2 General Description of the Numerical Experiment

The first step in the numerical experiment is to develop 100 paired synthetic vertical profiles of atmospheric ozone and water vapor (how the profiles are developed is discussed later in this chapter). These profiles are used as "true" profiles (**X** on p. 14). In other words they are considered to be the profiles as they actually appear in the atmosphere.

The second step is to run all 100 synthetic water vapor and ozone profiles through a forward model (see appendix A for discussion of forward model) which yields 100 synthetic water vapor ozone and brightness temperature spectra (**Y** on p. 14). These spectra are what the MAS instrument would measure when scanning the atmosphere described by the associated true profile.

In the process of creating these synthetic spectra, the forward model accesses two control files. These control files tell the forward model what values to assign to certain parameters. Among these parameters are the "true" values of the angular offset and the sideband ratio (included in **b** on p. 14). When these parameters are defined in the forward

model control files, the resulting spectra have the attributes defined by these parameters (Fig 4.1a).

The spectrum is then run through an inverse model (see appendix B for discussion of the inverse model). The inverse model takes the measured spectrum and computes a vertical profile of the associated constituents using the inversion technique known as "optimal estimation". These profiles represent the inversion algorithm's best estimate of the actual atmospheric behavior.

The inverse model accesses two different control files in the process of retrieving the appropriate profile. One of these control files contains initial estimates of the values expected for the sideband ratio and the angular offset (Fig 4.1b). The inverse model attempts to retrieve these parameters, as well as the vertical constituent profile.

The inverse model also requires two *a priori* profiles (one ozone and one water vapor) as additional inputs. When retrieving an ozone profile, the inverse model requires a water vapor *a priori* to remove the influence of the atmospheric water vapor spectrum from the measured ozone spectrum (see companion gas problem in Chapter 2). The *a priori* ozone profile serves as an initial estimate of the desired ozone profile.

4.3 Generation of True Profiles

This section describes the two different methods used to develop the true profiles used in the experiment. The results obtained using each method are discussed in Chapter 5.

18

(4.1a)

Control Files — Temperature Model, Pressure MZodel, True Value of Sideband Ratio, True Value of Angular Offset, Antenna Pattern, Filter Function, Other Model Parameters

"True" Ozone Profile → Forward Model ← Ozone or Water Vapor Spectra

"True" Water Vapor Profile →

(4.1b)

Control Files — Temperature Model, Pressure MZodel, Estimated Value of Sideband Ratio, Estimated Value of Angular Offset, Antenna Pattern, Filter Function, Other Model Parameters

Ozone (Water Vapor) Spectrum → Inverse Model ← Ozone (Water Vapor) Profile

A Priori Water Vapor (Ozone) Profile →

Fig 4.1 Flow Chart for Forward and Inverse Model

19

4.3.1 Scale Height Method

A program developed by the MAS science team is used to generate fifty true ozone and fifty true water vapor profiles (see appendix B for the program). Fifty profiles were generated to insure a good statistical sample. This program prompts the user to input the amplitude, altitude, and scale height of a major and, if applicable, minor peak as well as a smoothing parameter based upon the assumed vertical resolution of the instrument. The following equation is then used to compute a smoothed profile with volume mixing ratio values every 0.5 kilometers from the surface to 100 kilometers:

vmr(i) = A$_e$ x exp [- abs(alt(i) - maxvmr/H)] + A$_s$ x exp [- abs(alt(i)-minvmr/H$_s$)] **[4.1]**

Here **vmr(i)** is the volume mixing ratio (VMR) value (expressed in parts per million-volume (ppmv)) at the altitude **alt(i)**, **A$_e$** is the major peak amplitude, **maxvmr** is the altitude of the major peak, **H$_e$** is the scale height of the major peak, **A$_s$** is the amplitude of the minor peak, **minvmr** is the altitude of the minor peak, and **H$_s$** is the scale height of the minor peak.

The resulting profile has the expected shape of a "normal" ozone profile (Fig 4.2) . Ozone usually shows exponential growth up to the peak (usually located between 30-45 kilometers, with VMR values between 6-10 ppmv) and then an exponential decay above the peak to about 80 kilometers. Then there is a slight increase in VMR above 80 kilometers. [Bevilacqua et al, 1990; Gunson, 1990] The growth above 80 kilometers is not included in the profile because the retrieval algorithm reports only the values between 17-80 kilometers. Increases above that level do not play a major factor in the calculations.

The "normal" water vapor profile is very different from what the program produces. Above the peak of the water vapor profile (usually around 50-70 kilometers, with

Original Profile
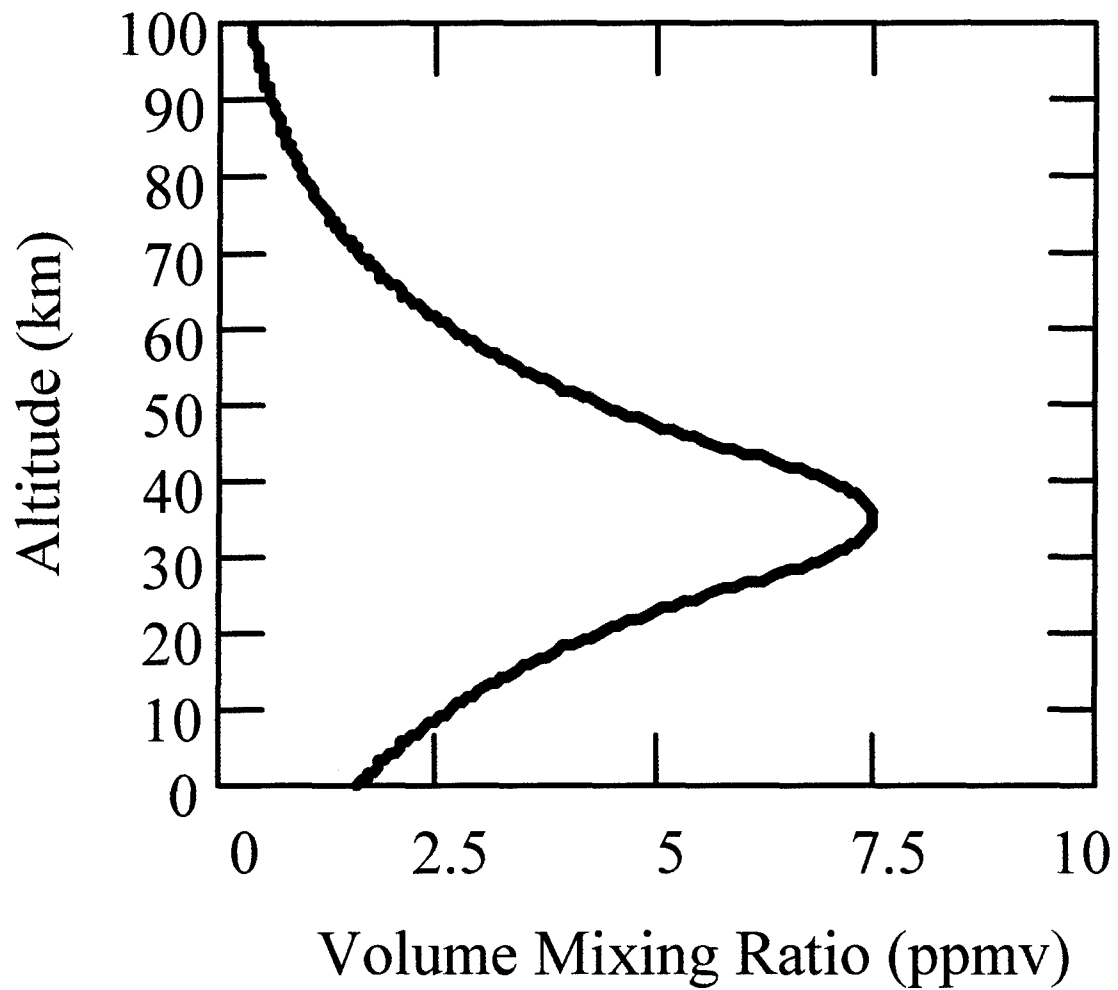
Fig 4.2 Profile generated using "original" profile program

VMR values near 5-8 ppmv) the VMR usually shows exponential decay. Below the peak, water vapor mixing ratios show a slow decay down to the hygropause (the minimum water vapor value which occurs around 16-20 kilometers with VMR values between 2-4 ppmv). Below the hygropause is rapid growth with VMR values above 10,000 ppmv near the surface (Fig 4.3).[Chiou et al, 1993; Gunson et al, 1990; McCormick et al, 1993; Bevilacqua et al, 1983; Bevilacqua et al, 1990]

Changes were made to the program in an effort to better match the shape of the calculated water vapor profile to the shape of a more natural looking water vapor profile. Two exponential functions were added to the original program. One takes into account the exponential growth below the hygropause and the other slows the decay between the hygropause and the peak. Although a few of the profiles had unusual shapes (Fig 4.4), most of the profiles were very reasonable (Fig 4.5). The VMR magnitudes produced were all reasonable regardless of the shape of the profile. The results obtained when these profiles were used as the true water vapor and ozone profiles are surprising (see Section 5.4).

4.3.2 Deviation Method

A set of 100 water vapor and 100 ozone profiles were generated using a different method than the one presented in Section 4.3.1. The assumption that the ozone and water vapor profiles retrieved at Table Mountain Observatory, California on March 30, 1992 (Fig 4.6 and 4.7) are representative of the global mean profiles is the basis for the method developed.
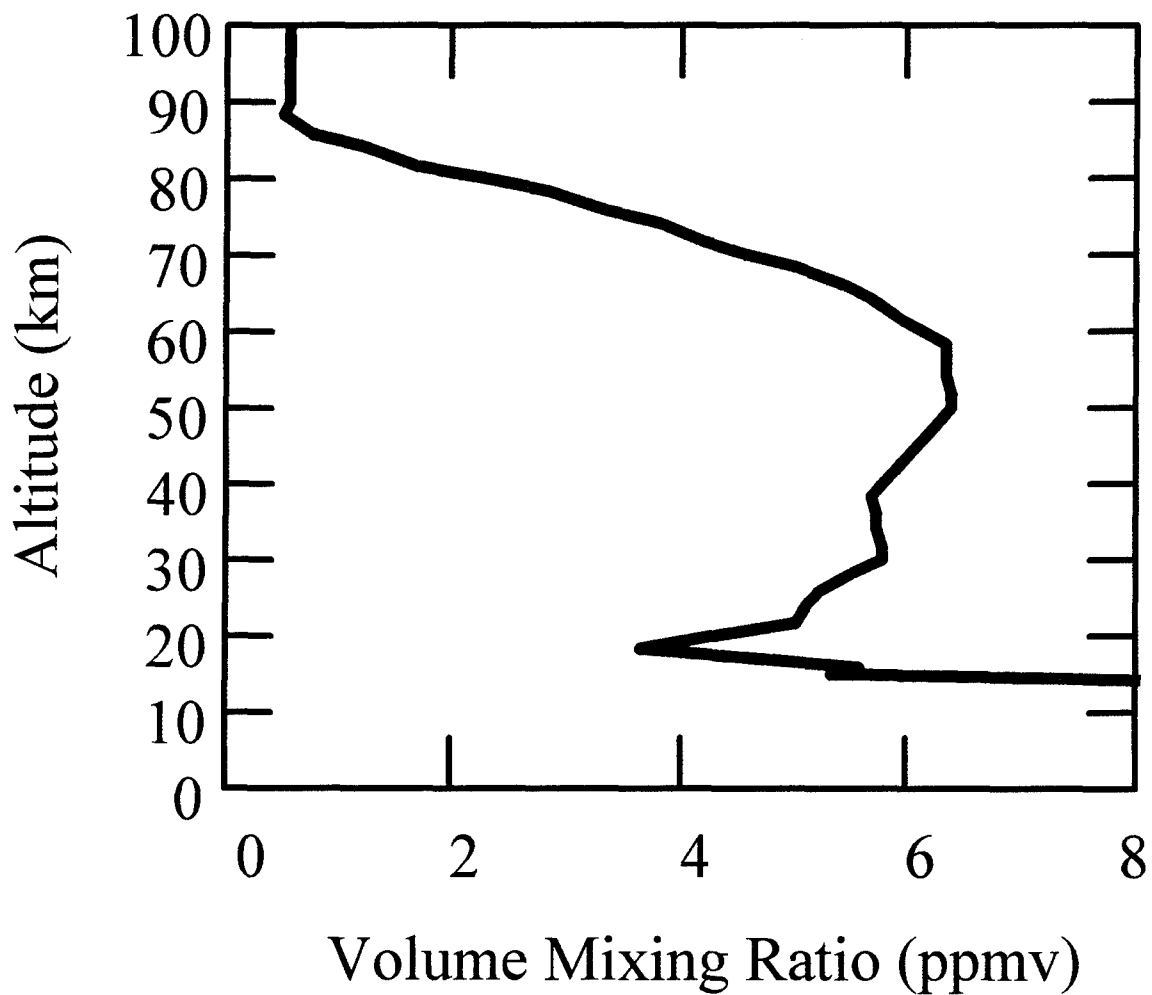
Fig 4.3 "Normal" Water Vapor Profile
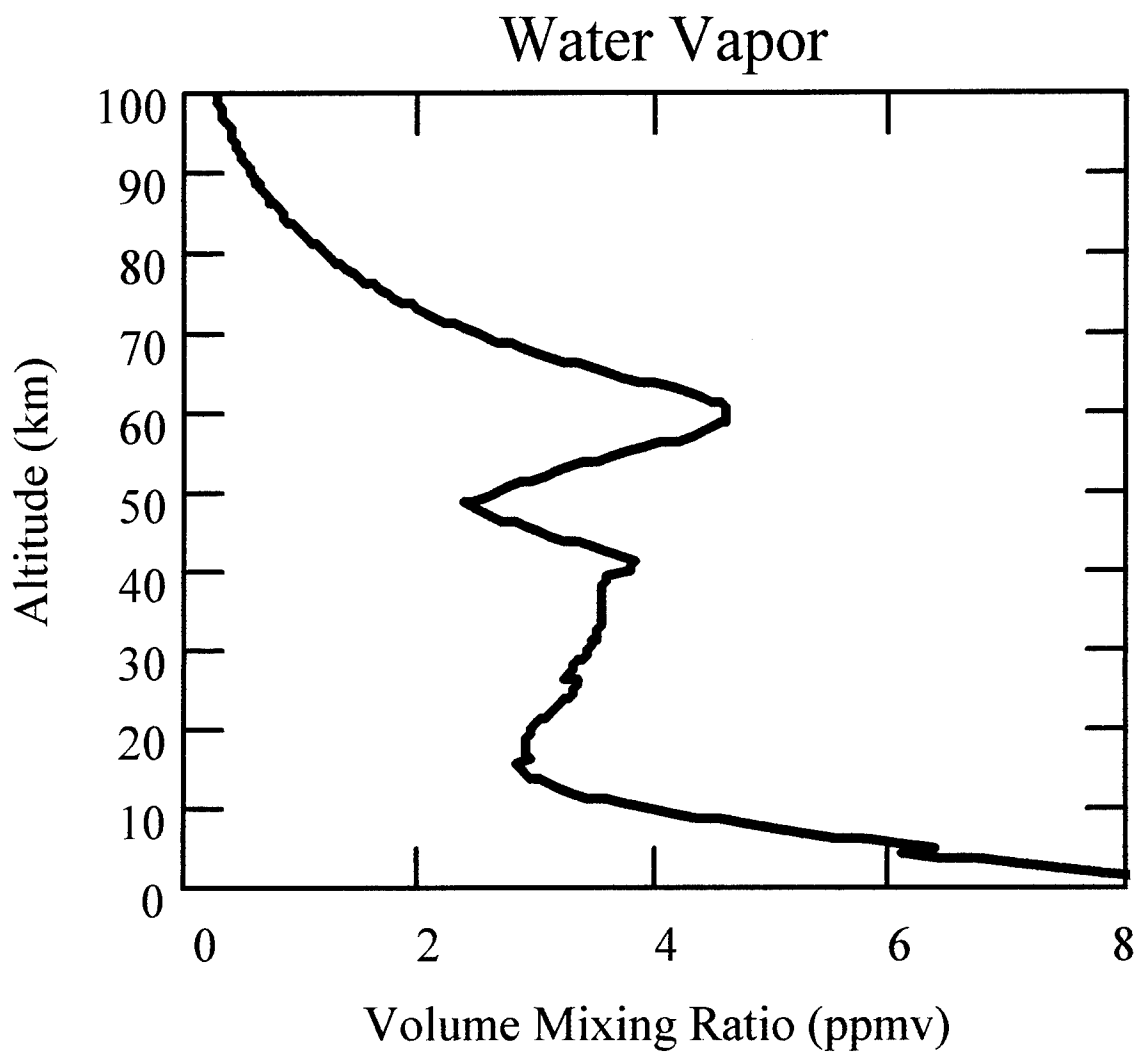
Water Vapor

Fig 4.4 Unusually Shaped Water Vapor Profile. Note the extreme drying near 50 km.

Nearly Normal Water Vapor Profile
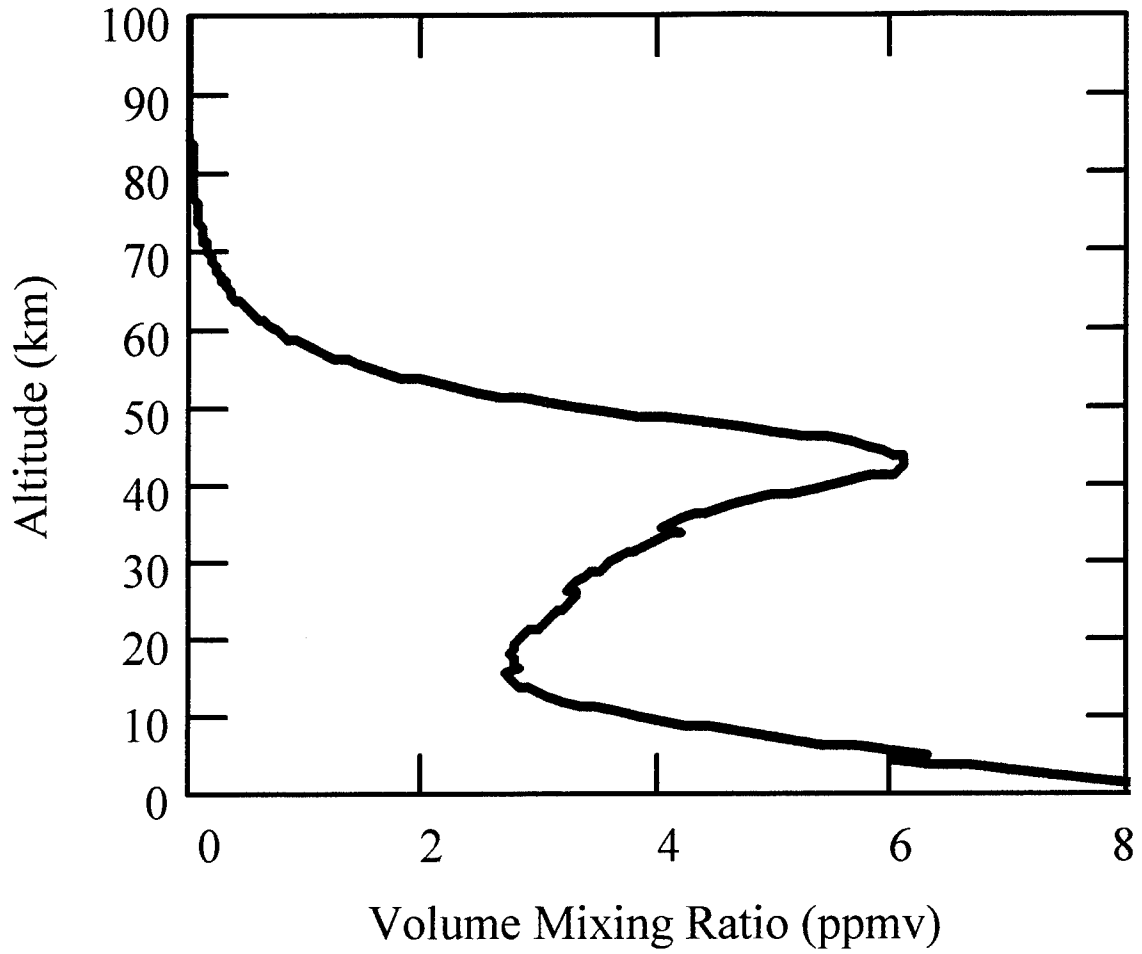
Fig 4.5 Water Vapor Profile with Nearly "Normal" Shape.

Ozone A Priori Profile
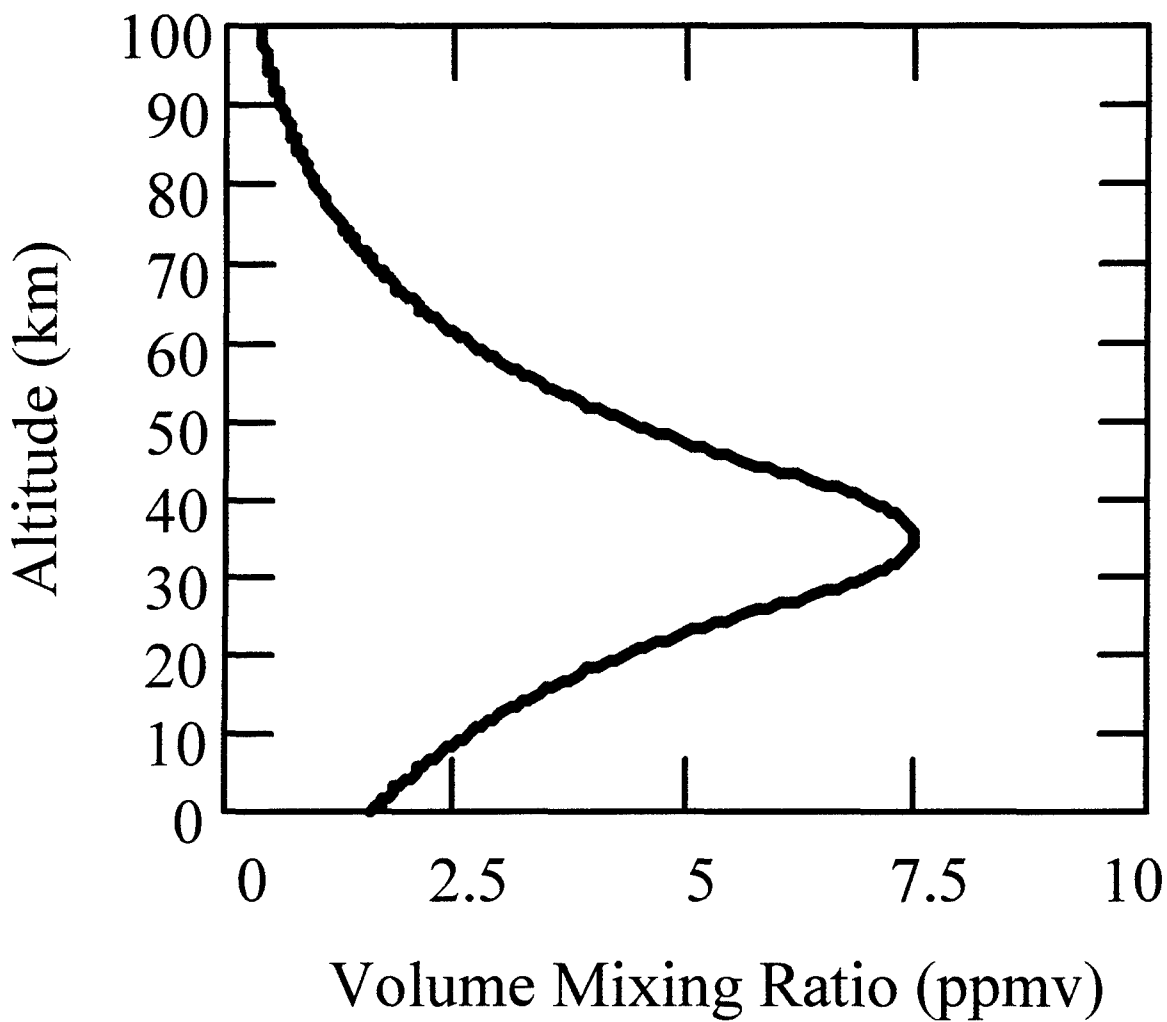
Fig 4.6 Ozone *A Priori* Profile Read at Table Mountain California.

Water Vapor A Priori Profile
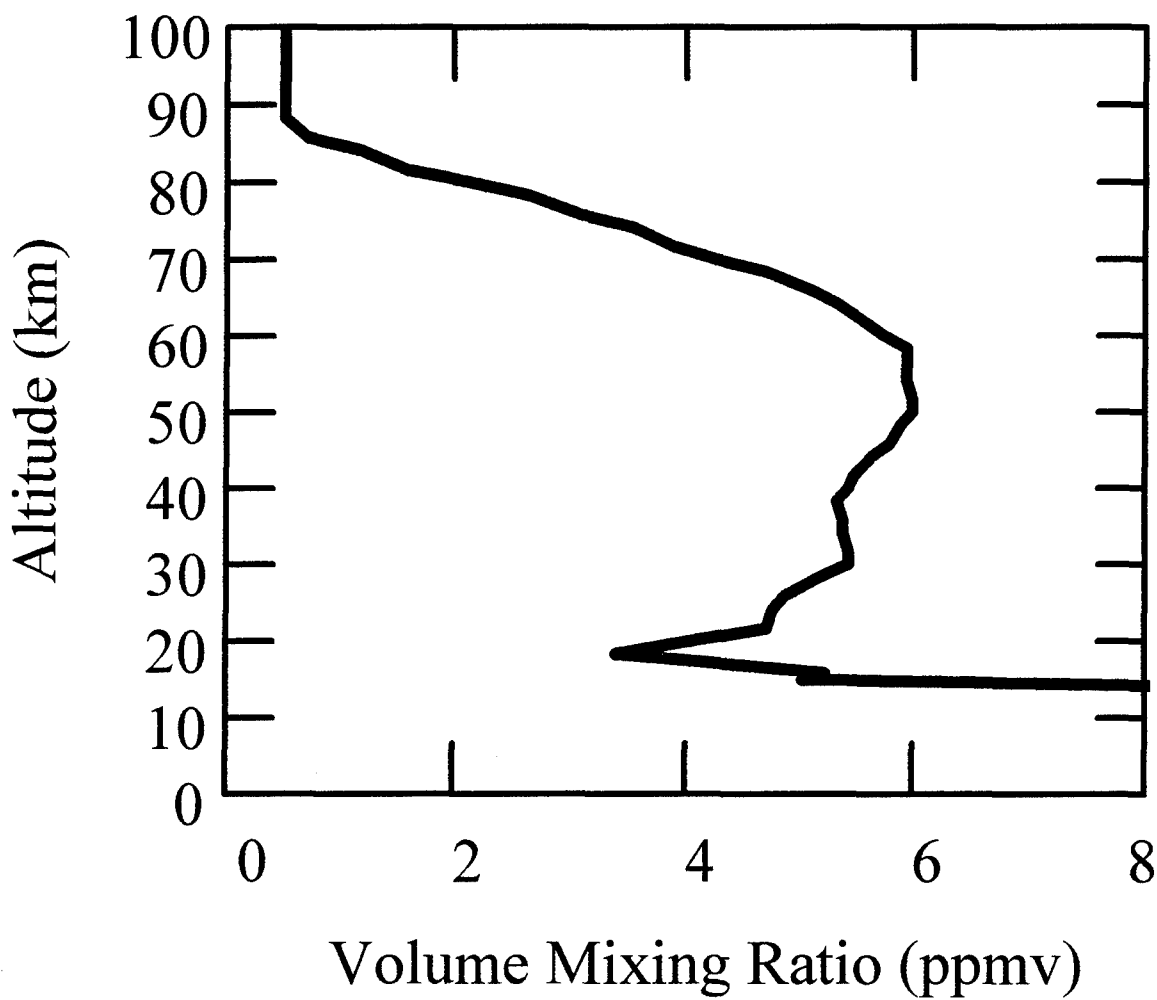
Fig 4.7 Water Vapor *A Priori* Profile Read at Table Mountain California.

A requirement of the numerical experiment is that the generated true profiles need to have the same basic shape and not depart too far from the Table Mountain retrievals. The experiment also required that the ensemble mean true water vapor and true ozone profiles are equal to the Table Mountain profile associated with each constituent. This allows the Table Mountain profiles to be considered the global climatological mean of the generated true profiles. These requirements are met by deviating the amplitude of the entire profile and the altitude of the peak VMR values of the Table Mountain profiles.

The following equation is used to manipulate the Table Mountain profiles:

$$newvmr(i) = (1 + (A \times \cos(pekalt - z))) \times ppmv(i) \qquad [4.2]$$

where **newvmr(i)** is the newly computed VMR value at altitude **i**, **A** is the amplitude determined by a random number being multiplied by 0.15 for the first fifty profiles of each constituent and 0.30 for the last fifty, and the altitude of the peak VMR of the Table Mountain profile is represented by **pekalt**. The variable **Z**, used to create a deviation in the altitude of the peak, is defined by a random number multiplied by 5 for fifty profiles of water vapor and ozone and 10 for the next fifty of each constituent (see appendix D for the program).

The random number generator provides an ensemble of values having a gaussian distribution centered around zero with a standard deviation of one [Press et al, 1993]. This distribution ensures that the mean deviation of both the altitude of the peak and the amplitude of the generated profiles will be zero. The result is that the ensemble mean profile of the generated true profiles of water vapor and ozone is the same as the profiles retrieved from Table Mountain.

4.4 Companion Gas Procedures (3 Cases)

The three different procedures used in the investigation of the error in the retrieved ozone profiles are described in this section.

4.4.1 Case 1: Ozone Retrievals Using the True Water Vapor Profiles

The first set of ozone retrievals uses true water vapor profiles and the climatological mean ozone profile as *a priori* inputs. This result gives the baseline from which to determine all other error contributions. If the true water vapor profile is used as the *a priori*, no error is introduced into the retrieved ozone profile that is attributable to an incorrect specification of the vertical profile of water vapor in the atmosphere . In other words, any ozone profile generated using this technique will not contain errors induced from the companion gas problem (Fig 4.8a).

4.4.2 Case 2: Ozone Retrievals Using the Climatological Mean Water Vapor Profile

The next trial retrieves the ozone profiles using fixed water vapor and ozone *a priori* profiles from measurements taken at Table Mountain Observatory during the time the ATLAS-1 mission was flown. These two fixed *a priori* profiles were assumed to represent the global climatological means of water vapor and ozone during the ATLAS-1 mission [Goldizen, 1995]. The procedure (which was described in section 4.3.2) used to develop the 100 true water vapor and 100 true ozone profiles ensures that these fixed *a priori* profiles are also the ensemble mean profiles of each constituent (Fig 4.8b).

Forward Model

$$F(X_{WT}, X_{OT}) \longrightarrow Y_W$$

$$F(X_{WT}, X_{OT}) \longrightarrow Y_O$$

X_{WT} and X_{OT} are the true water vapor and ozone profiles (100 of each) respectively.
Y_W and Y_O are the water vapor and ozone spectra respectively (100 of each).
F is the forward model.

Inverse Model

(4.8a)

$$I(X_{Oa}, X_{WT}, Y_O) \longrightarrow X_{ROT}$$

I is the inverse model.
X_{Oa} is the climatological mean ozone *a priori* from Table Mountain.
X_{ROT} is the retrieved ozone profile using the true water vapor profile as an *a priori*.

(4.8b)

$$I(X_{Oa}, X_{Wa}, Y_O) \longrightarrow X_{ROa}$$

X_{Wa} is the climatological mean water vapor *a priori* from Table Mountain.
X_{ROa} is the retrieved ozone profile using the climatological mean water vapor profile as an *a priori*.

(4.8c)

$$I(X_{Oa}, X_{Wa}, Y_W) \longrightarrow X_{RW}$$

$$I(X_{Oa}, X_{RW}, Y_O) \longrightarrow X_{ROR}$$

Y_W is the true water vapor spectrum.
X_{RW} is the retrieved water vapor profile.
X_{ROR} is the retrieved ozone profile using the retrieved water vapor profile as an *a priori*.

Fig 4.8 A Schematic Representation   of the 3 Experimental Procedures

4.4.3 Case 3: Ozone Retrievals Using the Retrieved Water Vapor Profiles

The water vapor profiles are subsequently retrieved using the climatological mean water vapor and ozone profiles as *a priori*. These retrieved water vapor profiles, along with the climatological mean ozone profile, are then used as the *a priori* for the retrieval of 100 ozone profiles (Fig 4.8c).

4.5 Root Mean Square Error Calculation

To determine the error contribution of an incorrectly specified water vapor profile on an ozone retrieval, the root mean square error (RMSE) between the volume mixing ratios of the retrieved ozone profiles and their associated true ozone profiles for the three cases are compared at three kilometer height intervals. The RMSE is expressed as a percentage of the climatological mean ozone profile to allow comparison with Rodgers' error analysis method. The RMSE calculation used all 100 ozone profiles from each of the three cases: those profiles retrieved using the climatological mean, retrieved, and true water vapor profiles, as the *a priori* during the inverse model run.

4.6 Error Calculations using Rodgers' Error Analysis

Rodgers' error analysis is another method used to investigate the error introduced into the retrieved ozone profile by using the retrieved or climatological mean water vapor profiles, instead of the true water vapor profile as the *a priori*, in the ozone retrieval. This same result can be obtained by subtracting the RMSE values associated with a true water vapor *a priori* from the RMSE curve associated with the retrieved and the climatological

mean water vapor profiles as the *a priori*. The results from these two methods are compared in section 5.5.3.

In the Rodgers' approach, a perturbation matrix (D_b) is used to compute the errors resulting from the use of different *a priori* water vapor profiles. The matrix represents the sensitivity of the retrieved parameter to perturbations in a non-retrieved parameter.

$$[D_b]_{i,j} = \frac{\partial X_{OR}}{\partial X_{Wa}} = \left[\frac{\partial (X_{OR})_i}{\partial (X_{Wa})_j} \right] \qquad [4.3]$$

Here X_{OR} is the retrieved ozone profile and X_{Wa} is the non-retrieved parameter matrix which, in this case, is the climatological mean water vapor *a priori* profile, i and j range from 1-22 (the total number of levels in the retrieval). Since each profile consists of 22 atmospheric levels, D_b is a 22 x 22 matrix in which column j represents a change in the retrieved ozone when the water vapor *a priori* is perturbed at level j.

D_b was created by changing VMR values in X_{Wa} and retrieving a new ozone profile using the same ozone spectrum and the new X_{Wa} as the *a priori*. The newly retrieved ozone profiles were then subtracted from the ozone profile retrieved using the original unperturbed climatological mean *a priori*. The altitudes in the original X_{Wa} which correspond to retrieved altitudes (22, 26, and 32 kilometers) were each increased by 5%. If a retrieved altitude is not specifically defined in the *a priori* (17,23, and 35 kilometers) the inverse model interpolates a VMR value from the values associated with the nearest altitudes above and below the desired altitude. In this case, the values nearest to the altitude were increased by 5%. For example to perturb the VMR value at 17 kilometers, the VMR values at 16 and 18 kilometers were increased by 5%.

To compute the covariance matrix needed to find the error in question, a difference matrix must first be defined:

$$d_R = X_{RW} - X_{WT}$$ [4.4]

$$d_a = X_{Wa} - X_{WT}$$ [4.5]

Where the columns of d_R represent the difference vector resulting from the subtraction of the retrieved water vapor profile (X_{RW}) from the true water vapor profile (X_{WT}). d_a is a matrix whose columns are the vector difference between the *a priori* water vapor profile (X_{Wa}) and the true water vapor profile (X_{WT}).

The two difference matrices defined above are used to find the values which define the elements of the covariance matrices. The covariance matrices were developed using the following equations

$$(S_R)_{(i,j)} = \overline{(d_R)_{(i,n)} \times (d_R)_{(j,n)}} - (\overline{d_R})_{(i,n)} \times (\overline{d_R})_{(j,n)}$$ [4.6]

$$(S_a)_{(i,j)} = \overline{(d_a)_{(i,n)} \times (d_a)_{(i,n)}} - (\overline{d_a})_{(i,n)} \times (\overline{d_a})_{(j,n)}$$ [4.7]

Here i and j range from 1 to 22 (the total number of levels in the retrieval) and n ranges from 1-100 (the total number of compared profiles). The result is two 22 x 22 matrices.

The following matrix equation is used to find the errors in question:

$$S_{bR} = D_b S_R D_b^T$$ [4.8]

$$S_{ba} = D_b S_a D_b^T$$ [4.9]

S_{bR} is the ozone error introduced through the use retrieved water vapor profile as the *a priori* instead of the true water vapor profile. S_{ba} is the ozone error introduced through the use of the climatological mean water vapor profile as the *a priori* instead of the true water vapor profile. The square root of the diagonals of these matrices represents the differences

between the RMS error of the ozone retrieved using the true water vapor and the RMSE of the ozone retrieved using one of the other two methods. For comparison to the RMSE method, the values found in using Rodgers' error analysis method are expressed as a percentage of the climatological mean ozone profile.

4.7 Angular Offset and Sideband Ratio Procedures

Following are the procedures used to investigate how accurately the inverse model retrieves the angular offset ($\delta\theta$) and sideband ratio (**R**): in the control files for the forward model the "true" values for the sideband ratio and angular offset are defined. In the control files for the inverse model, initial estimates for these parameters were based on values determined by the Naval Research Lab during antenna calibration tests (for $\delta\theta$) and from early retrieval results (for **R**). The ensemble mean of 100 retrieved values for each parameter is then statistically analyzed and the results are compared to the known true value for each parameter.

CHAPTER 5

Experimental Results

5.1 Introduction

This chapter presents the results obtained from the experimental procedures described in the previous chapter.

5.2 Angular Offset Results

The value of the true angular offset used in the generation of the water vapor and ozone spectra is -0.07 degrees. This value was determined to be the actual angular offset after studying approximately two hundred retrieved spectra from the MAS ATLAS-1 mission. In the inverse model, the initial estimate assigned for the value of the angular offset was -0.10 degrees. This value was based upon a lunar calibration experiment of ATLAS-2 (April 1993) as well as careful review of pre-launch antenna pattern measurements [Goldizen, 1995].

The 100 water vapor and 100 ozone retrieved angular offsets were statistically analyzed, both separately and together to quantify to what degree the inversion algorithm was able to recover the correct value for this parameter (-0.07), given that our initial estimate for it was somewhat larger (-0.10).

For the water vapor retrievals, the mean value of the angular offset is -0.07099 degrees and the standard deviation is 0.00391 degrees. The resulting error between the actual value and the average retrieved value is 1.5%. The values are normally distributed around the mean value (Fig 5.1). The apparent discrepancy in the value between the

Angular Offset of Water Vapor
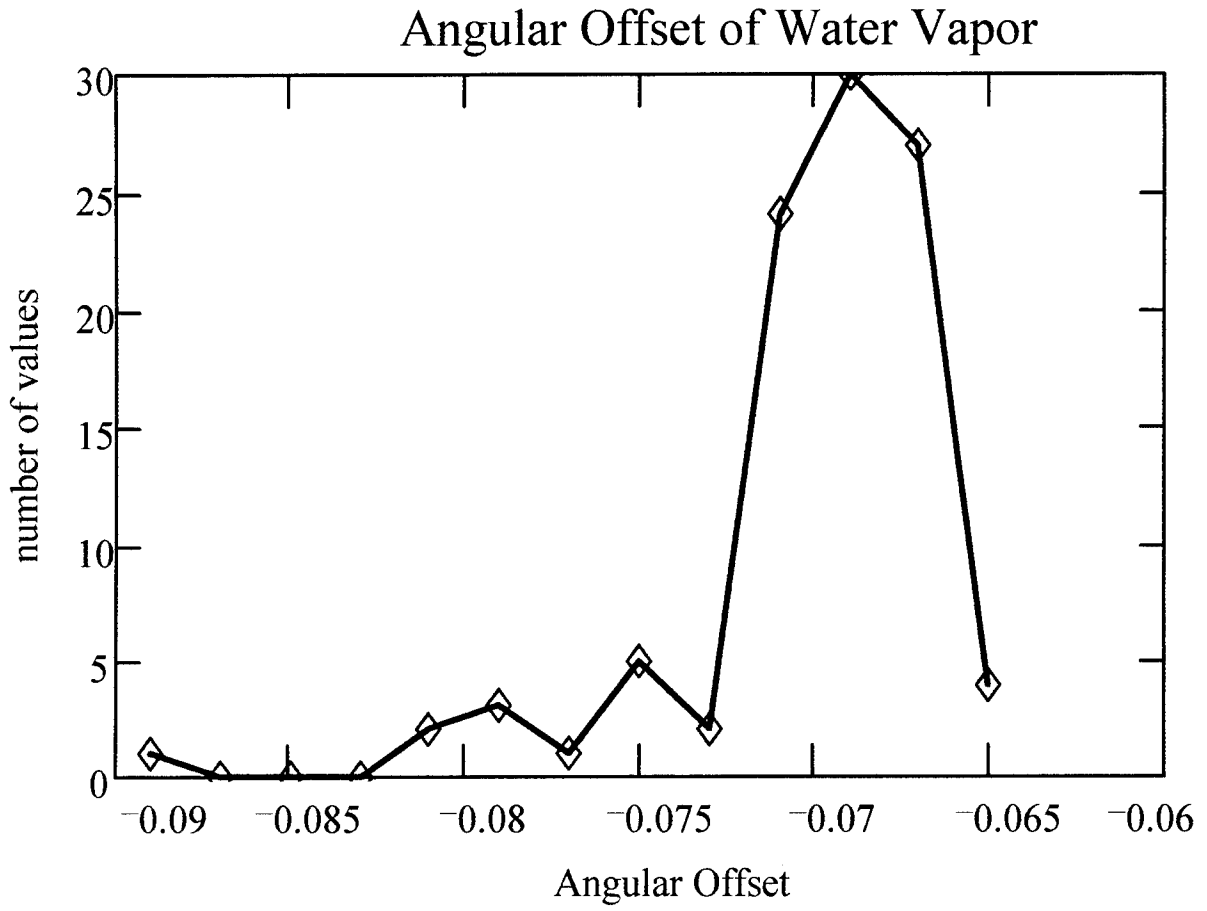
Fig 5.1 Distribution of Angular Offset Values From Water Vapor Retrievals.

distribution mean and the computed mean has to do with the binning algorithm used to create the distribution.

The mean value of the angular offset retrieved from the 100 ozone retrievals is -0.07079 degrees, an error of 1.1%, with a standard deviation of 0.00585 degrees. The distribution is once again normally distributed around the computed mean (Fig 5.2), and the discrepancy between the computed and distribution mean results from the binning algorithm.

When both water vapor and ozone retrievals are included in the same calculation, the result is an average retrieved angular offset of -0.07089 degrees and a standard deviation of 0.00453 degrees. The resulting error between the average retrieved offset and the actual offset is 1.3%. Once again the resultant distribution is a normal distribution around the computed mean value (Fig 5.3).

5.3 Sideband Ratio Results

The true value of the sideband ratio used to generate the synthetic spectra is 0.40. Like the angular offset, this value was also determined from the nearly two hundred retrievals recovered from the ATLAS-1 mission. 0.40 is thought to be the actual, or true, sideband ratio of the MAS instrument. In the retrieval algorithm, the instrument was initially assumed to have a pure double sideband mixer. This assumption requires the use of 0.50 as the sideband ratio estimate.
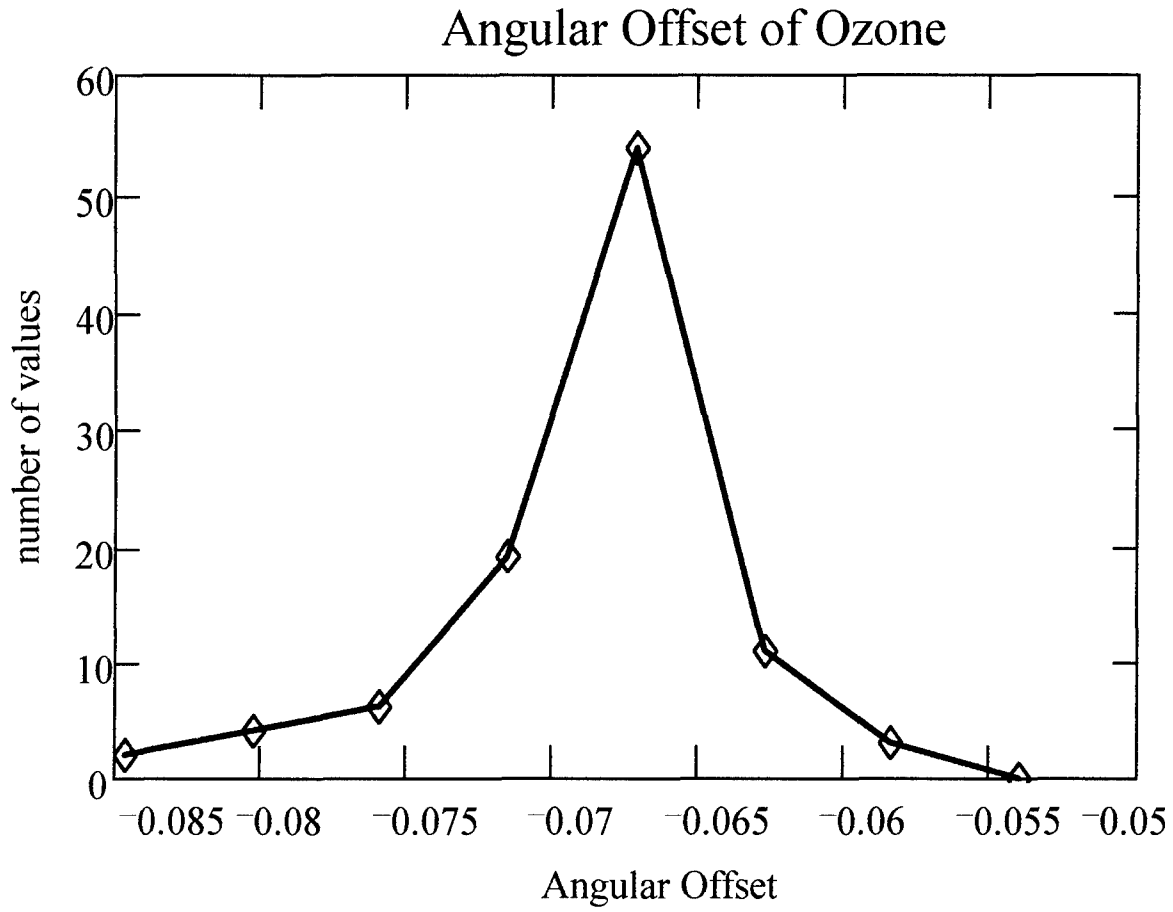
Fig 5.2 Distribution of Angular Offset Values From Ozone Retrievals.
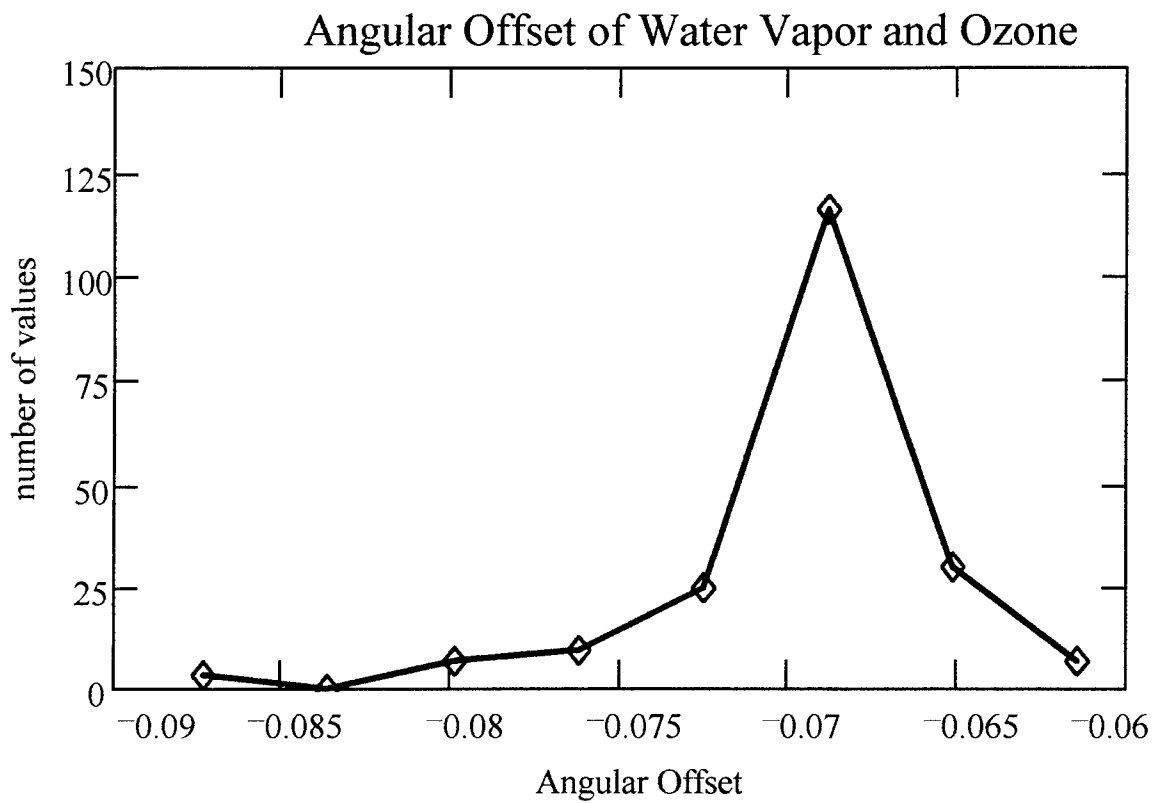
Fig 5.3 Distribution of Angular Offset Values From Both Ozone and Water Vapor Retrievals.

The computed average retrieved sideband ratio for the water vapor retrievals is 0.40006 with a standard deviation of 0.00074. The error between the average retrieved value and the actual value is 0.01%. The distribution was approximately gaussian about the mean value (Fig 5.4).

For the ozone retrievals, the results are even better than those obtained for the water vapor case. The average retrieved sideband ratio is 0.40003, which results in an error of 0.007%, with a standard deviation of 0.00468. The distribution of values is once again approximately a gaussian distribution about the mean value (Fig 5.5).

Combining both the water and ozone retrievals, the average retrieved sideband ratio is 0.40005, resulting in an error with respect to the actual value of 0.01%. The standard deviation is 0.00340 with a normal gaussian distribution (Fig 5.6).

5.4 Results From Using the Profiles Generated by the Scale Height Method

The results obtained when the profiles used were those generated by the method described in section 4.3.1 are surprising. When the spectra associated with these profiles were run through the inverse model using the climatological mean for the *a priori* (case 2 section 4.4.2), the RMS errors are on the order of 15-30%. At first it was thought that the unusually shaped profiles were responsible. However, the RMS errors associated with some of the most reasonably shaped profiles are on the order of 25%. Because of these huge errors these profiles are not included in the final results. The profiles generated using the method described in section 4.3.2 are used instead. Possible reasons for the
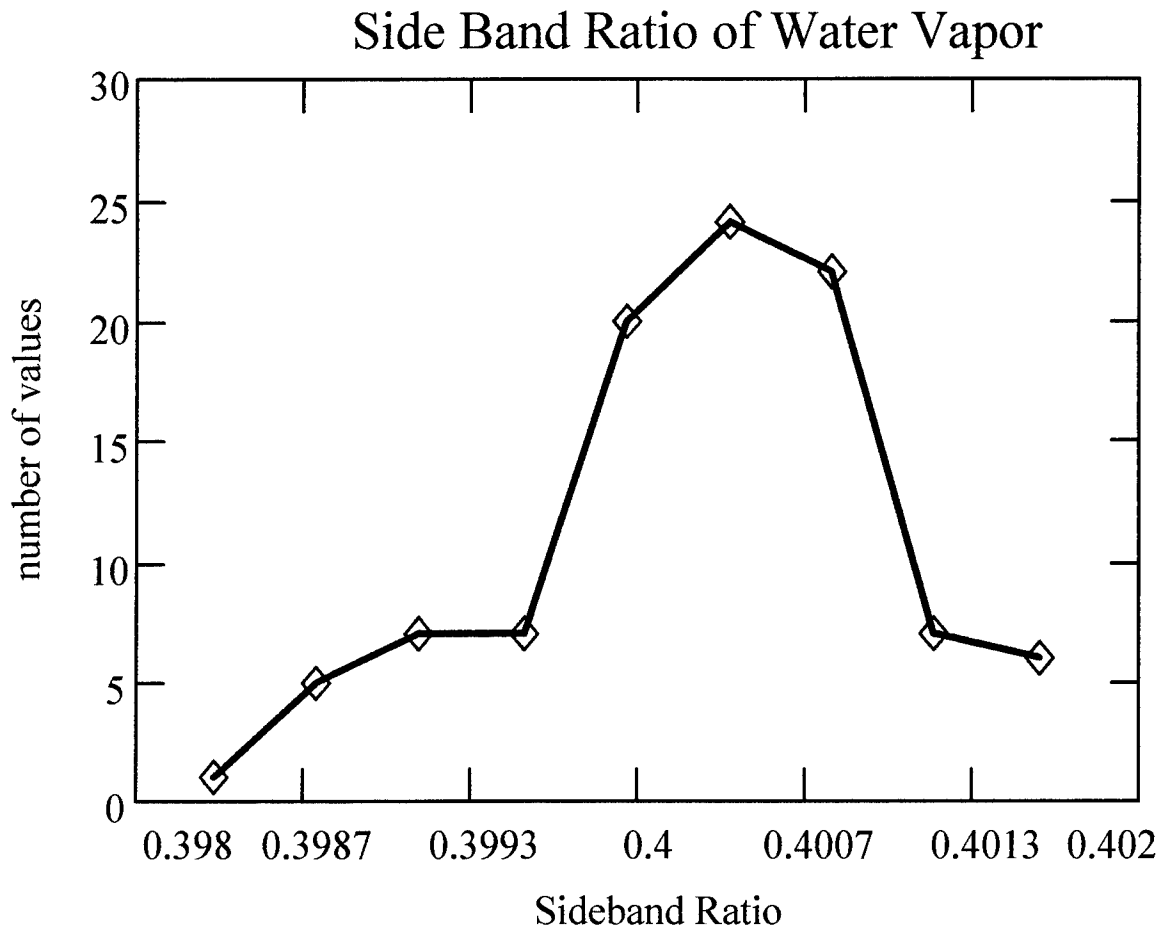
Fig 5.4 Distribution of Sideband Values From Water Vapor Retrievals.

Side Band Ratio of Ozone
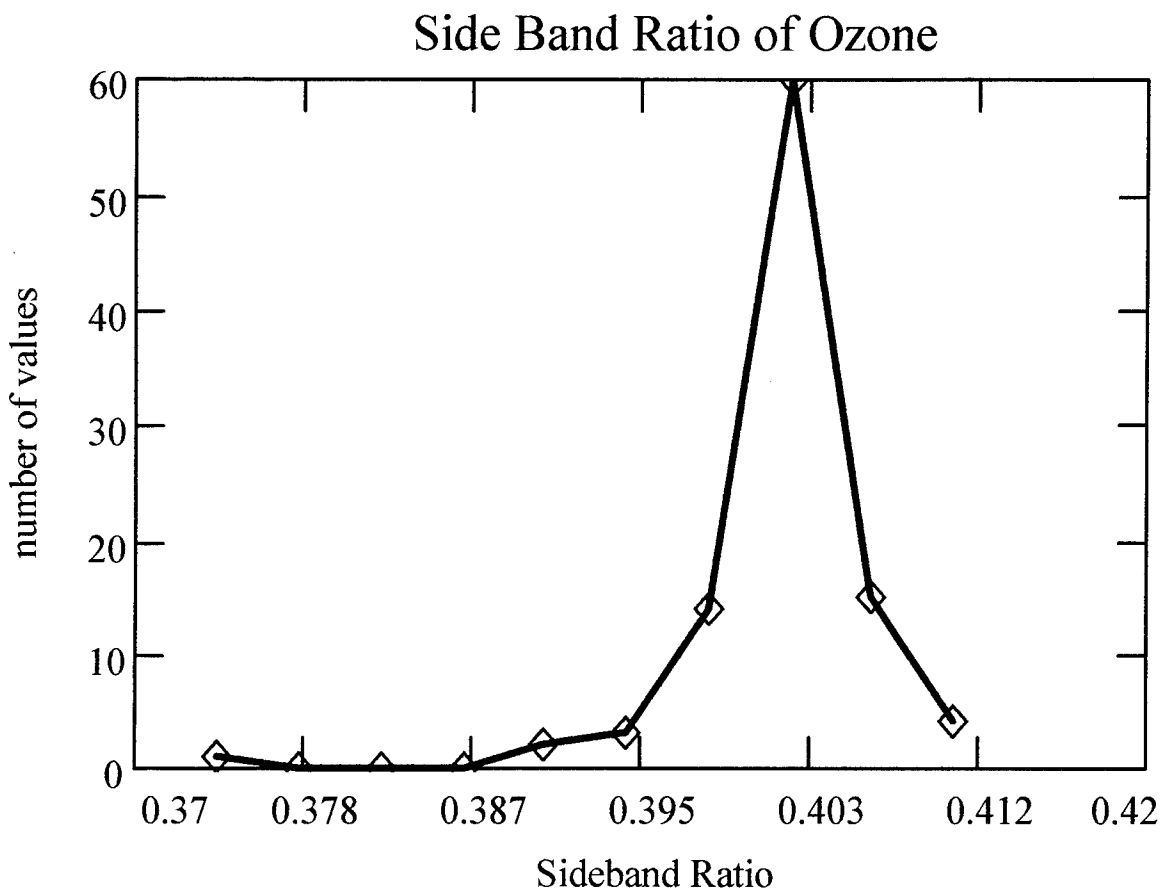
Fig 5.5 Distribution of Sideband Values From Ozone Retrievals.
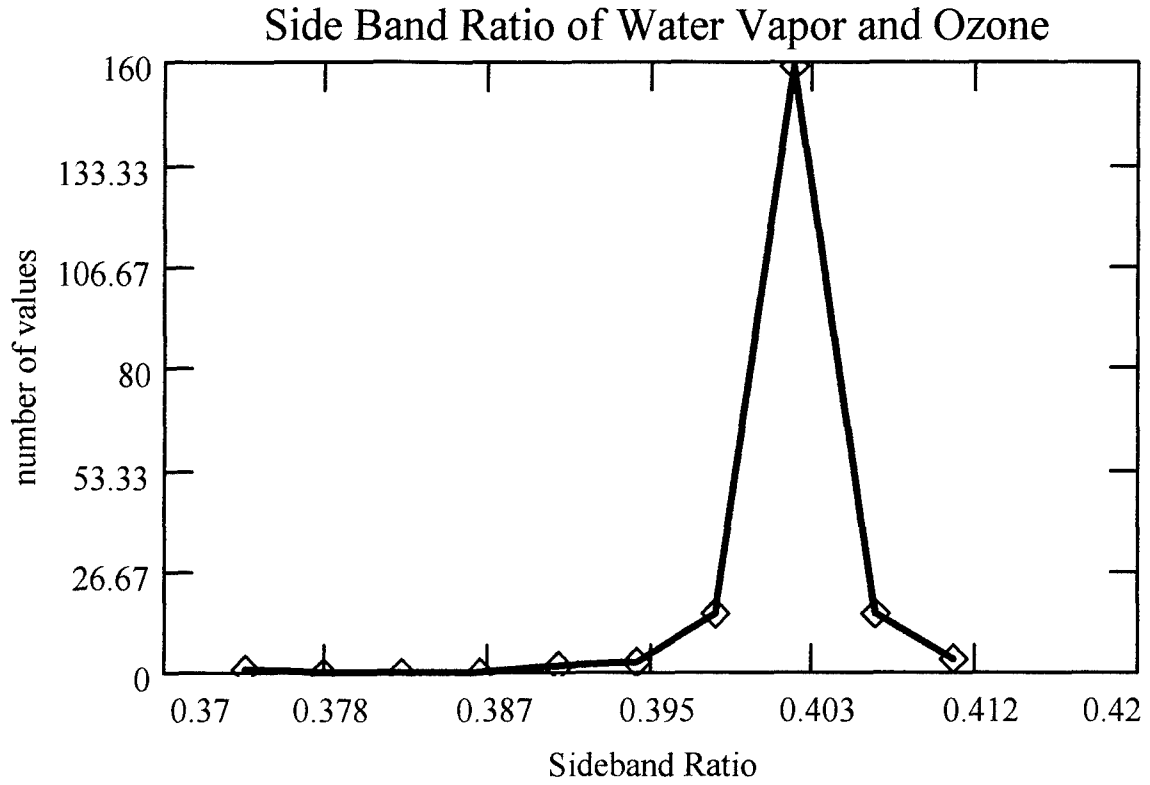
Fig 5.6 Distribution of Sideband Values From Both Water Vapor and Ozone Retrievals.

large errors resulting from the profiles generated using this method are discussed in Section 6.4.

5.5 Results of the Error Analysis of the Companion Gas Problem

This Section discusses the results obtained in the investigation of the companion gas problem using true profiles generated by the method described in section 4.3.1. Also, the two error analysis methods are compared.

5.5.1 Root Mean Square Error Results

The profiles developed by the procedure described in section 4.3.1 are run through the forward model to develop synthetic spectra. The measurement ozone spectra are then run through the inverse model using either the corresponding true water vapor, retrieved water vapor, or a climatological mean water vapor profile as the *a priori* (described in section 4.4 and figure 4.7). The RMSE between the retrieved ozone profile and the associated true ozone profile is calculated at 3 kilometer intervals at altitudes between 17-80 kilometers. This value is then expressed as a percent of the ensemble mean true ozone profile.

The first fifty ozone profiles (derived by using an amplitude variation of 15% with a 5 kilometer height variation) are compared first (Fig 5.7). As the figure shows, the errors above 38 kilometers are not significantly different. The plot becomes more variable below about 32 kilometers, which is just below the VMR peak.

Fig 5.7 RMSE Error From First 50 Profiles.

(Blue Trace: Retrieved H_2O as *A Priori*)
(Red Trace: Mean H_2O as *A Priori*)
(Green Trace: True H_2O as *A Priori*)

The ozone retrieval true water vapor curve has the lowest RMSE. This is expected: if the true water vapor profile is known the inverse model can remove the water vapor spectral contribution exactly so that the retrieved ozone profiles are unaffected by this error source. In an actual retrieval, however, the true water vapor is not known. This curve can be considered a baseline error trace.

Near the altitude of the VMR peak (30 km) the curve with the lowest RMSE is that for ozone retrieved using the retrieved water vapor as the *a priori*. At and below 28 kilometers the curve for ozone retrieved using the climatological mean water vapor profile has the lowest RMSE. This trace also has the lowest RMSE values above 34 kilometers. It should be noted that the differences between the RMSE values using the true water vapor *a priori* and either of the other curves are never greater than three percent.

The next plot shows the RMSE for the true profiles which are allowed to vary with a standard deviation of 30% in amplitude and 10 kilometers in peak VMR altitude (Fig 5.8). The shape of this error plot is nearly the same shape as the previous error plot. One distinct difference is that the RMS errors increase. This is not surprising since the true profiles are allowed more variation.

Near the average height of the peak (32 kilometers) the curve with the lowest RMSE is once again associated with the retrieval which uses the retrieved water vapor profile as its *a priori*. This curve continues to display the lowest error down to seventeen kilometers. The only exception is between 28 and 22 kilometers. In this altitude range, those retrievals using the climatological mean water vapor profiles as the *a priori* display
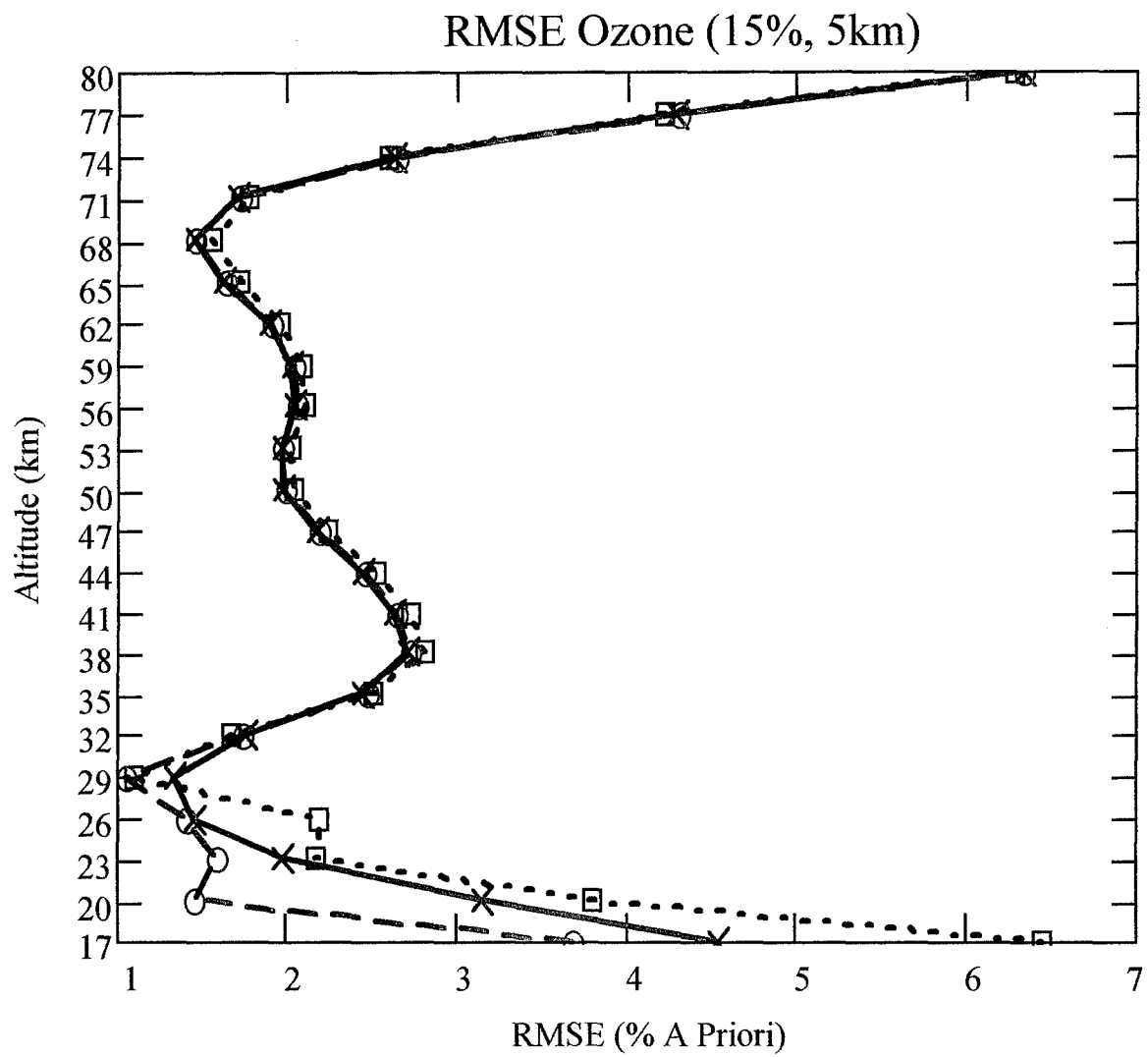
Fig 5.8 RMSE Error From Second 50 Profiles.

(Blue Trace: Retrieved H$_2$O as *A Priori*)
(Red Trace: Mean H$_2$O as *A Priori*)
(Green Trace: True H$_2$O as *A Priori*)

lower error value. Above 32 kilometers the retrieved and climatological mean water vapor cases are almost identical.

Finally, all one hundred retrievals are compared on one plot (Fig 5.9). The ozone retrieval which uses the retrieved water vapor profile as the *a priori* once again has the lowest RMSE near the altitude of the peak in VMR values. Between 28 and 22 kilometers the retrievals obtained using the climatological mean as the water vapor *a priori* has the lower RMSE. Below 22 kilometers the set of ozone retrievals which uses the retrieved water vapor as the *a priori* had the lower RMSE. Above 35 kilometers both curves are indistinguishable.

5.5.2 Rodgers' Error Analysis Results

Rodgers' error analysis computes the error introduced into a retrieved ozone profile because the *a priori* water vapor profile differs from the true water vapor profile. The errors computed are expressed as a percentage of the climatological mean ozone profile to facilitate the comparison between Rodgers' error analysis and the RMSE computed earlier.

The error trace computed from the ozone profiles using the climatological mean water vapor profile as the *a priori* has basically the same shape as the error trace for the ozone retrievals using the retrieved water vapor profile at the *a priori* (Fig 5.10 and Fig 5.11 respectively). The largest difference between the curves is 0.04% at 23 kilometers.

Three error peaks found at 20, 29, and 38 kilometers are apparent on both traces. It is not well known exactly what causes this periodic shape in the error curves. This

48

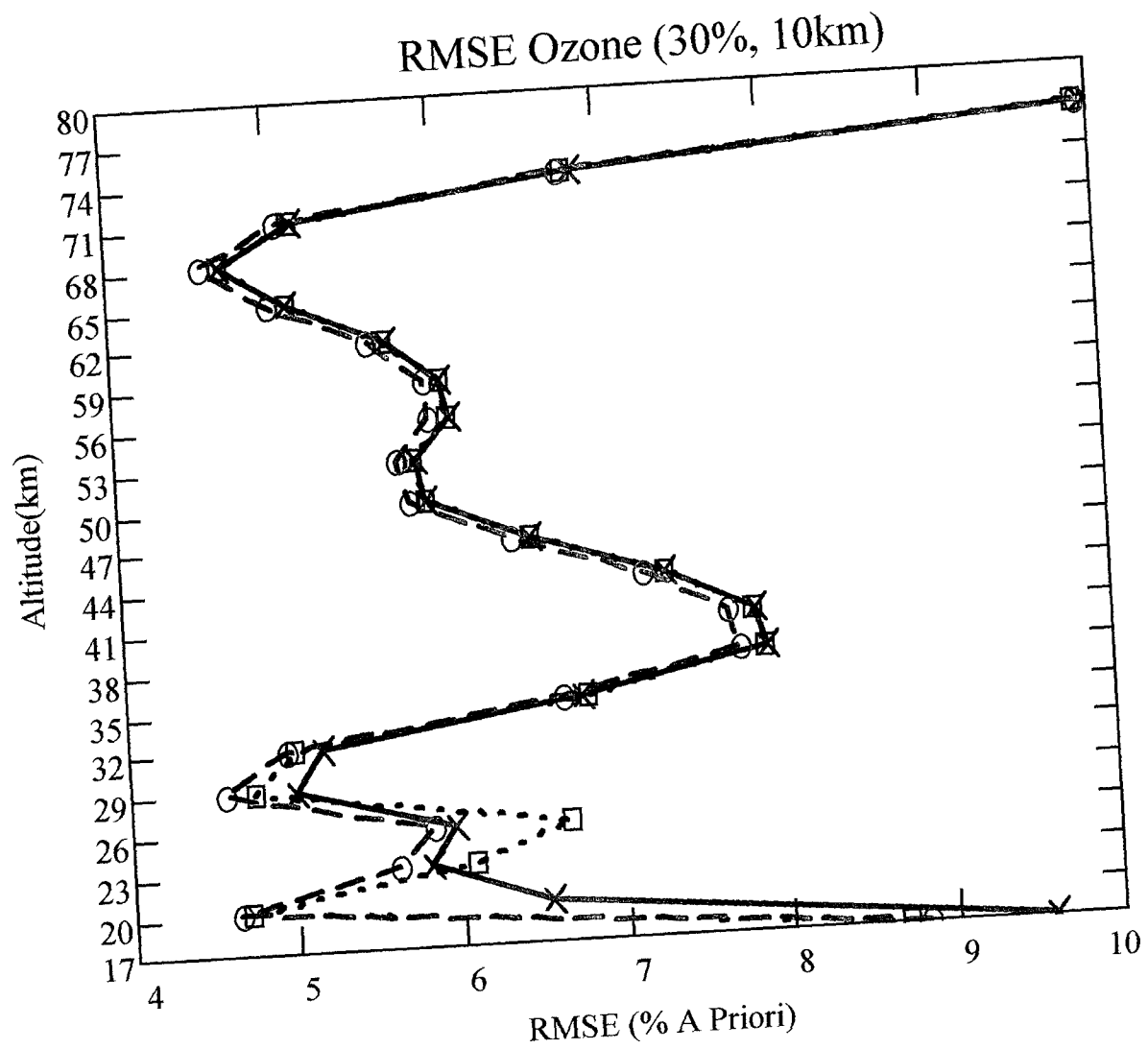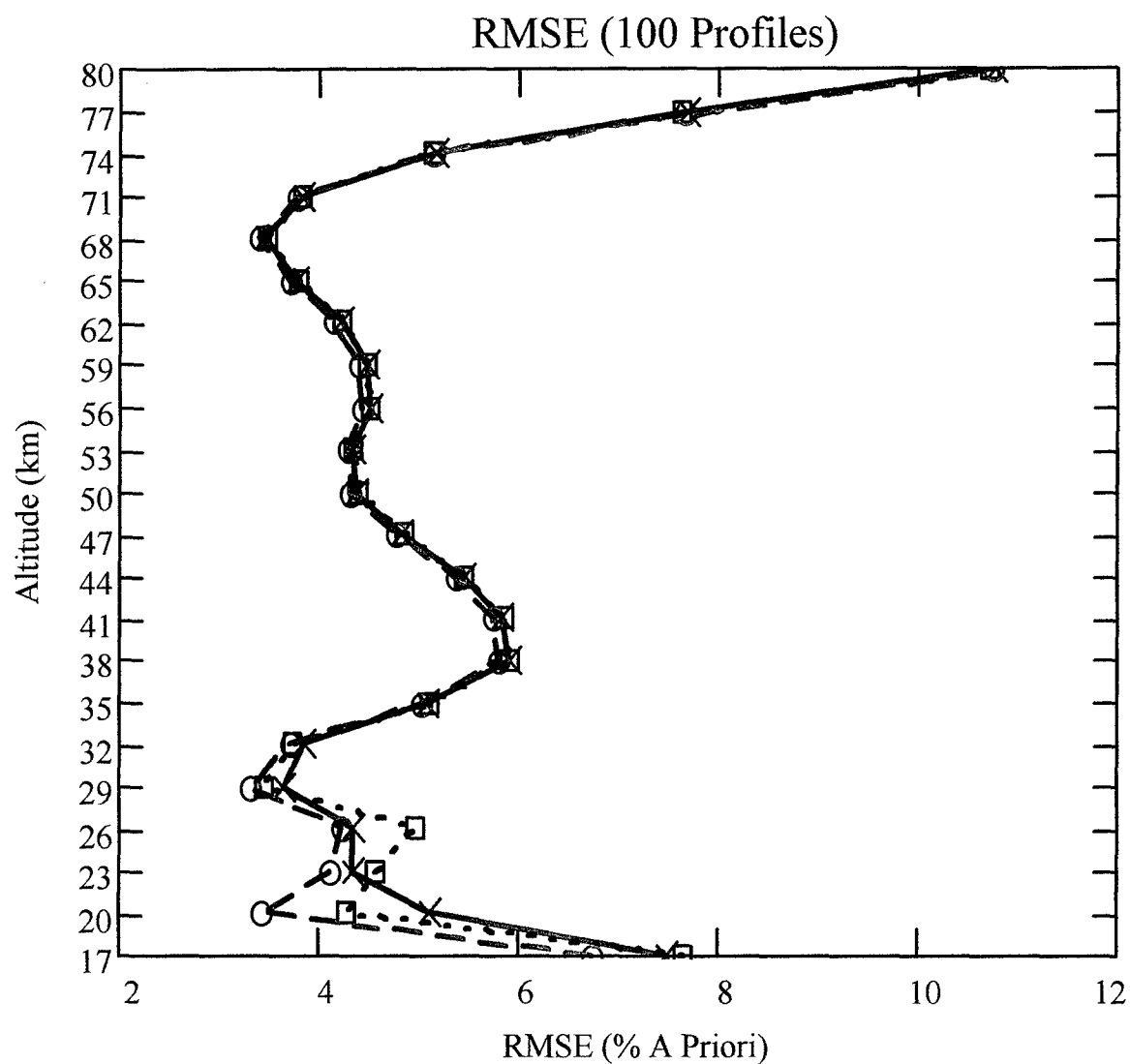**Fig 5.9** RMSE Error From All 100 Profiles.

(Blue Trace: Retrieved H_2O as *A Priori*)
(Red Trace: Mean H_2O as *A Priori*)
(Green Trace: True H_2O as *A Priori*)
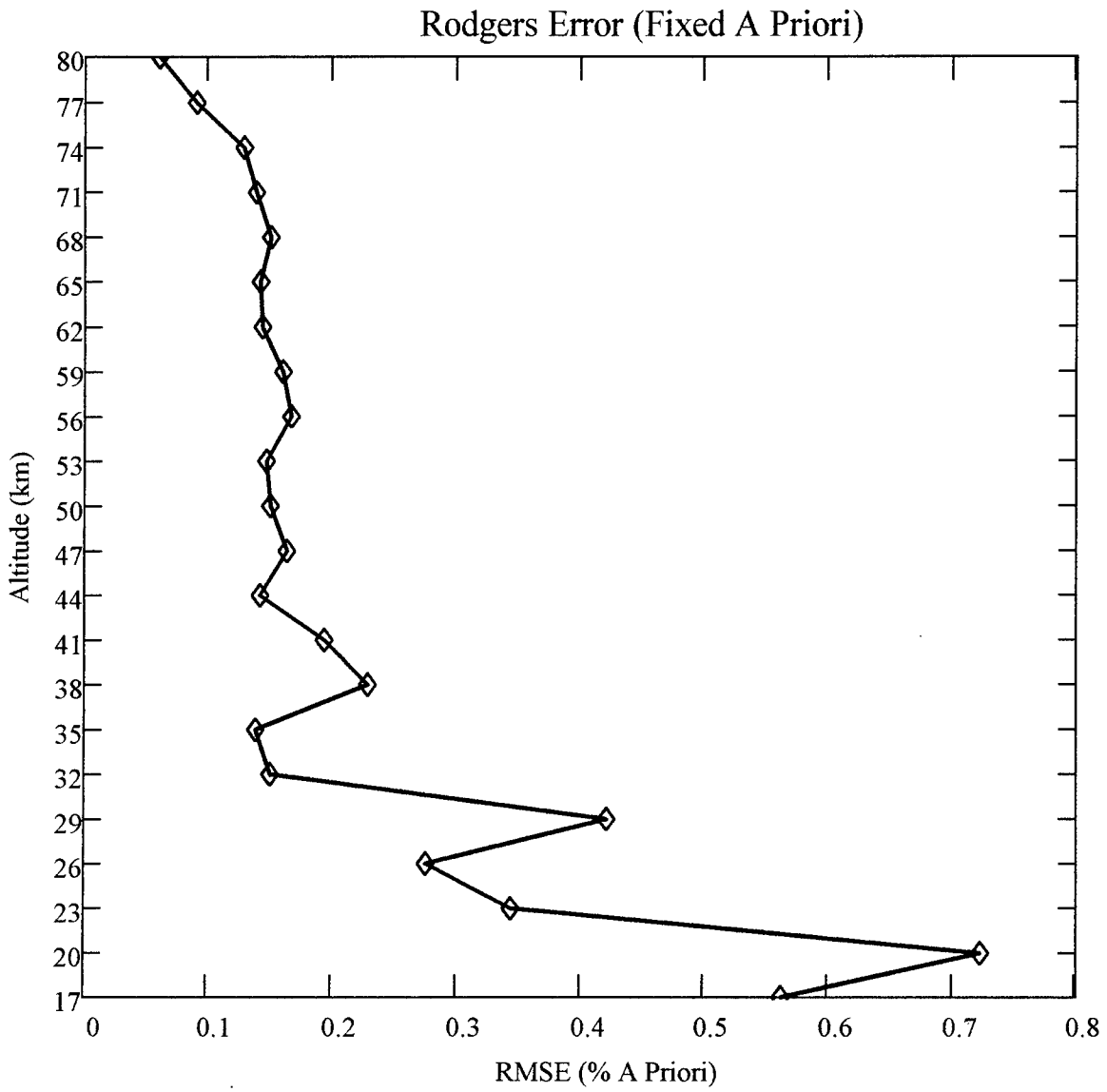
Fig 5.10 Analysis of Error Introduced by Using the Mean Water Vapor as the *A Priori*
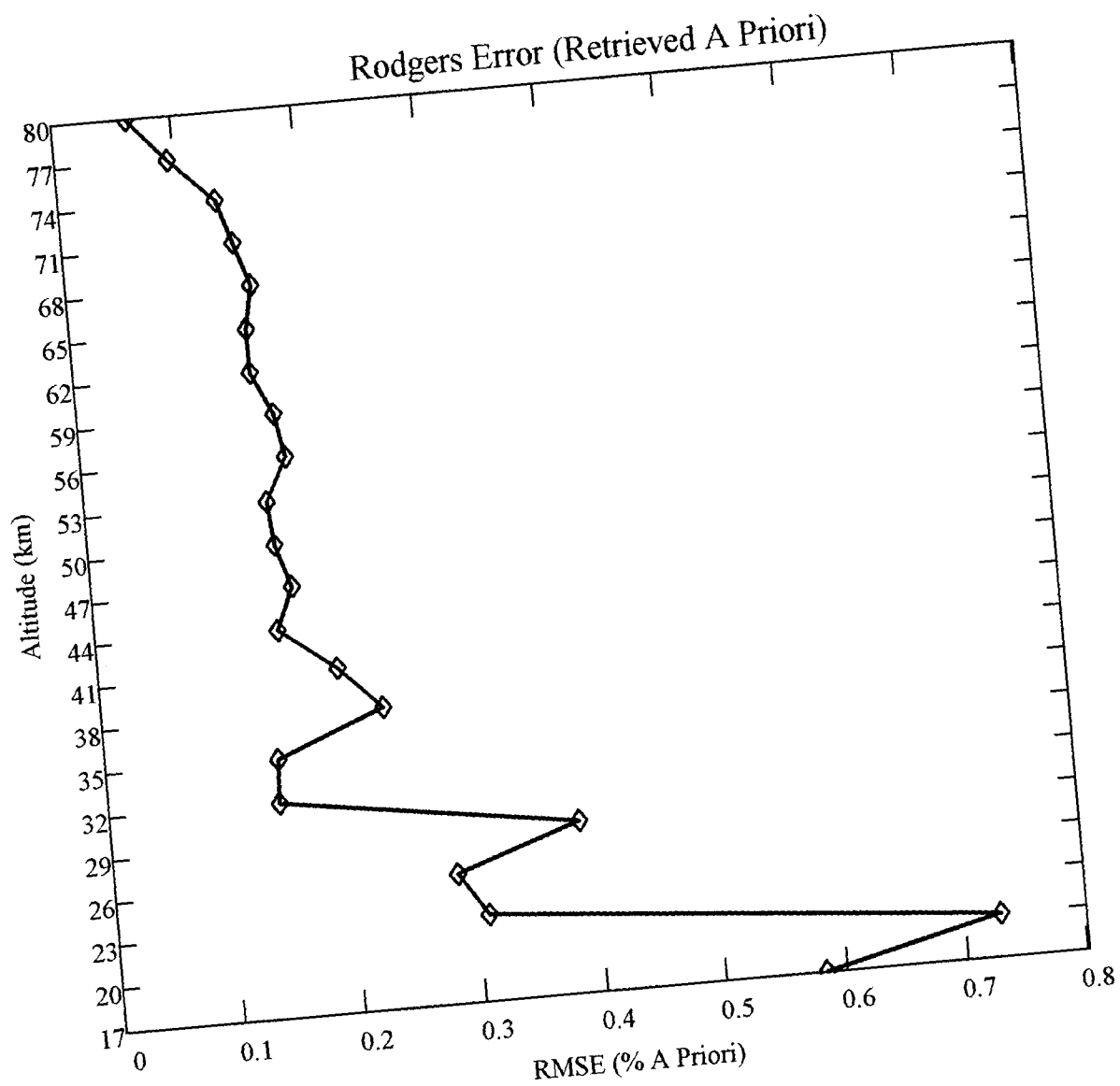
Fig 5.11 Analysis of Error Introduced by Using the Retrieved Water Vapor as the *A Priori* Instead of the True Water Vapor

oscillatory pattern was identified when Rodgers' technique was used in other MAS error analyses as well as in an unrelated investigation of stratospheric ozone using ground-based microwave observations [Connor et al, 1991].

5.5.3 Comparison of Rodgers and RMSE Results

To compare Rodgers' error with the RMSE approach, the RMS error of the ozone retrievals computed using the true water vapor profile as an *a priori* is subtracted from the RMSE of both the ozone retrievals which use the retrieved water vapor *a priori* and retrievals using a climatological mean water vapor *a priori*.

The RMSE and Rodgers' errors calculated from the retrievals using the climatological mean water vapor profile as the *a priori* have essentially the same shape (Fig 5.12). The errors computed from the ozone retrievals using the retrieved water vapor profile as the *a priori* are similarly shaped as well (Fig 5.13). The periodic pattern discussed in section 5.5.2 is also apparent in the RMSE curves, although one peak occurs at a different altitude in the case using a retrieved water vapor profile as the *a priori*. This would suggest that this oscillatory pattern is not an inherent result of Rodgers' technique, but may be a result of the mathematics of the inverse model itself.

The differences in the values of the RMSE and Rodgers' technique is the result of the different way the companion gas error is calculated for each case. For RMSE, the companion gas error was calculate as follows:

$$\sigma_{CG} = \sigma_R - \sigma_T \qquad [5.1]$$
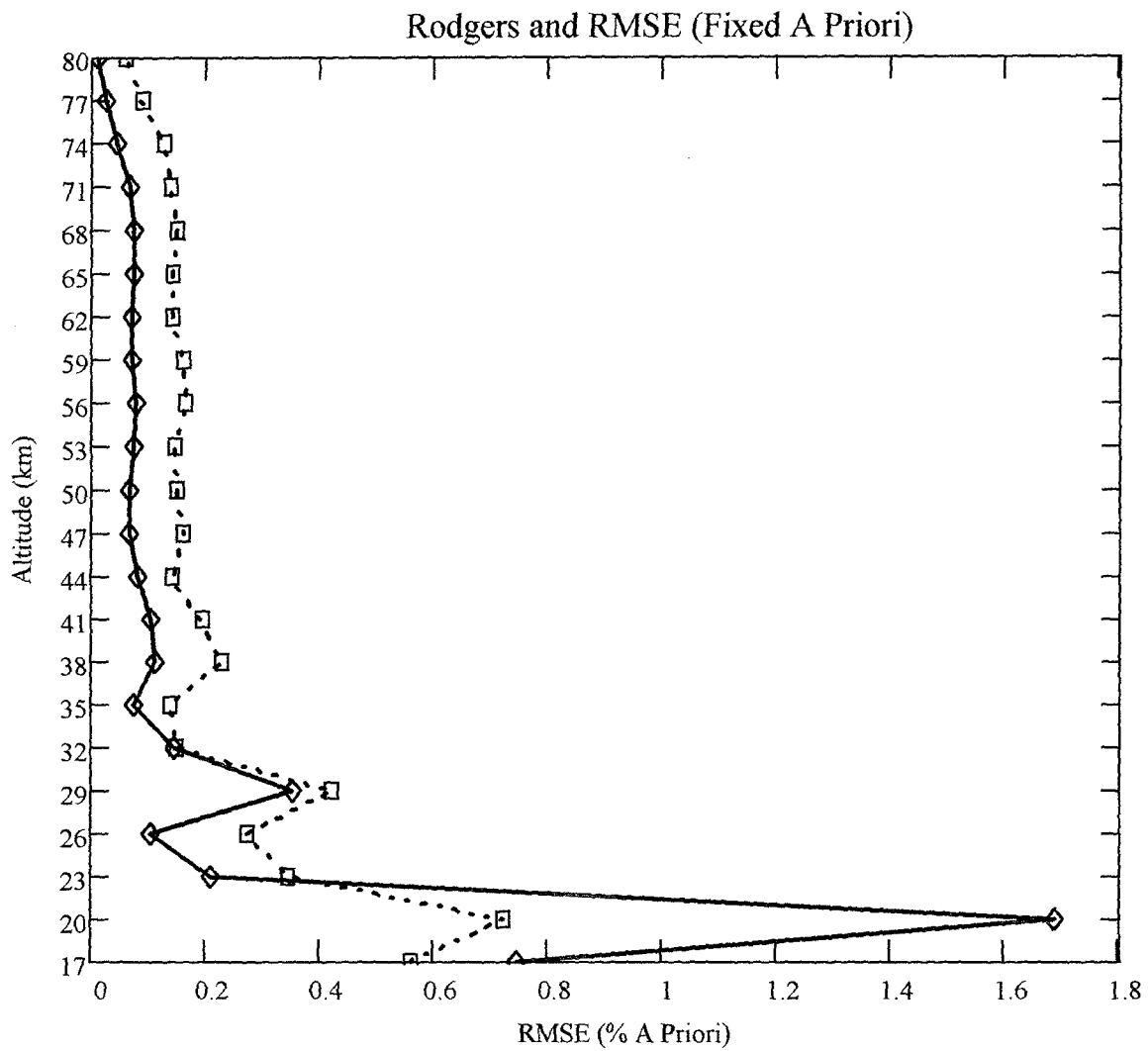
Fig 5.12 Comparison of RMSE (Red Curve) and Rodgers Error (Blue Curve) for a Fixed Water Vapor *A Priori*.

Rodgers and RMSE (Retrieved A Priori)
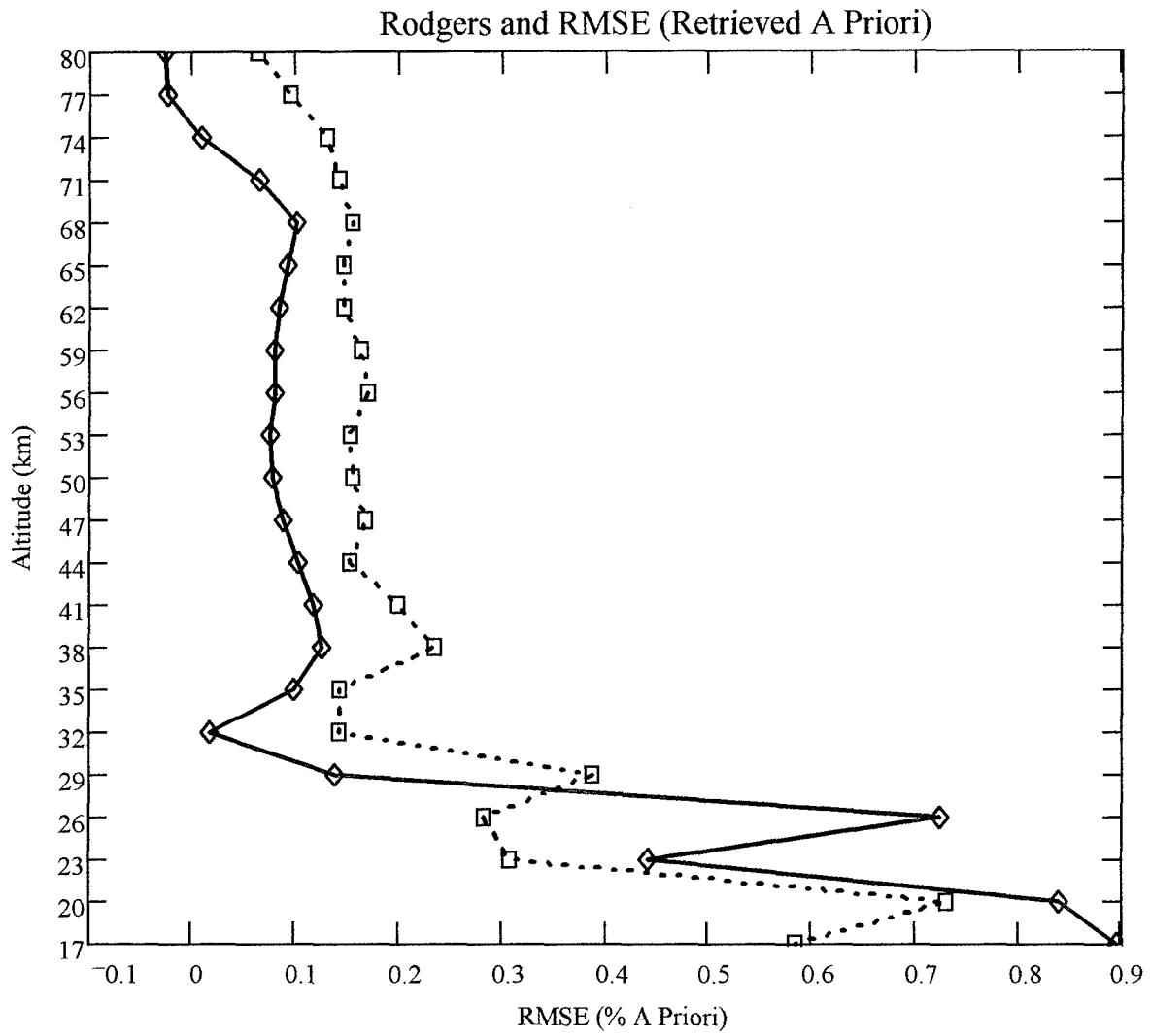
Fig 5.13 Comparison of RMSE (Red Curve) and Rodgers Error (Blue Curve) for a
Retrieved Water Vapor *A Priori*.

For Rodgers' error analysis the equation is slightly different:

$$\sigma_{CG}^2 = \sigma_R^2 - \sigma_T^2 \qquad [5.2]$$

Where σ_{CG} is the error from the companion gas problem, σ_R is the total error resulting from a retrieval of a profile of an atmospheric constituent, and σ_T is the total error less the companion gas error. It should now be obvious that the techniques may investigate the same type of error, but the values computed will be different.

CHAPTER 6

Conclusions

6.1 Introduction

Some of the conclusions which can be drawn from the results obtained in the experiment are presented in this chapter.

6.2 Angular Offset Conclusions

The results presented in section 5.2 show that the inverse model does an excellent job retrieving the angular offset from noise-free measured spectra. The errors were all less than 2% and the standard deviations were no more than 10% of the mean. Remembering that the distributions were essentially Gaussian, the results tell us that 68% of the retrieved values were well within 10% of the actual value (it is assumed that the mean of the distribution is an accurate estimate of angular offset). The retrieved values of the angular offset can be considered accurate. The value which deviated farthest from the actual value was -0.0879 degrees. This results in an error of 25.6%.

6.3 Sideband Ratio Conclusions

The sideband ratio retrieved by the inverse model was even more accurate than the retrieved angular offset values. The error between the average retrieved value for the sideband ratio and the actual value were all below 0.1%. 68% of the retrieved values

were within 2% of the actual value. The value farthest way from the mean was 0.3714, for an error of only 6.5%. The retrieved values of the side band ratio are extremely accurate and can be trusted.

6.4 Conclusions from Profiles Generated Using Scale Height Method

The resultant errors from the retrievals using the profiles developed from this method were on the order of 15-30%. The conclusion reached was that the inverse model might not be as robust as initially believed. If the true profile corresponding to a measured spectrum deviates too much from the *a priori* profile used in the retrieval, the inverse model does not retrieve a realistic profile.

Because noise-free spectra were used, the retrieval algorithm could have been too tightly constrained when trying to fit the retrieved profile spectrum (a spectrum which results when the retrieved profile is run through the forward model) to the measured spectrum within the error specified in one of the control files. The addition of noise to a spectrum can make it easier for the inverse model to retrieve a profile within the constraints stated in the control files (Fig 6.1).

The retrieval problem noted above did not occur in the nearly 200 retrievals of the ATLAS-1 data set, possibly because the data set included noise. Therefore, the MAS *a priori* values assumed for water vapor and ozone must have been relatively close to the actual atmospheric profiles at the time of the ATLAS-1 mission.

An area for further investigation is to find out for what values does a spectrum deviate too far from the *a priori* to allow for an acceptable retrieval. Is the altitude of the
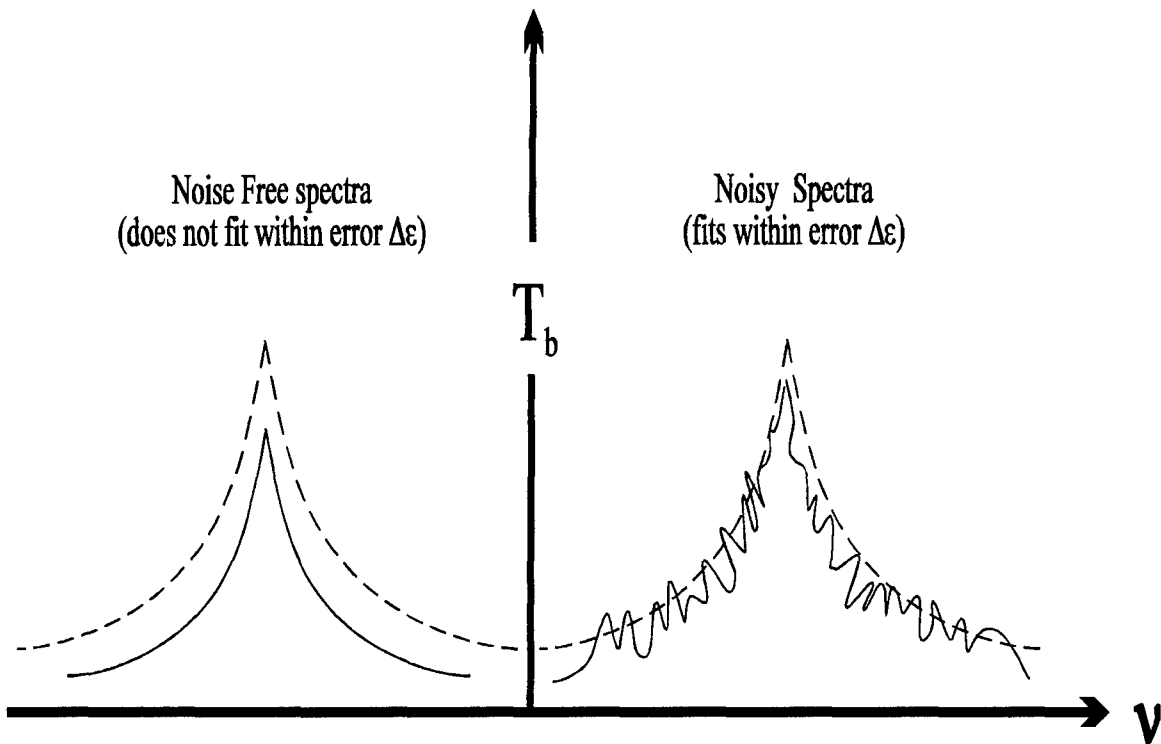
Fig 6.1 Figure Shows How a Spectrum With Noise Could Be Closer to the True Spectrum than a Noise-Free Spectra. The Solid Curves Represent the Measured Spectra While the Dashed Curves Represent the Retrieved Spectra.
(Not to Scale)

peak in the profile most important, or is it the shape of the profile which determines whether or not a spectrum can result in a good retrieved profile?

6.5 Companion Gas Conclusions

Both retrieval methods used, one using a retrieved water vapor profile (different for each retrieved ozone profile) the other using a climotological mean water vapor profile (fixed for all retrieved ozone profiles) as *a priori* profiles, retrieved the ozone profiles very accurately. The RMSE difference between the two methods is less than 1%. The Rodgers' error analysis difference is less than 0.5%. Which method is best depends on the part of the profile to be studied and the computational power or time available to the project.

If computer power or time is limited, the best method to use is that which uses the fixed climatological *a priori* water vapor profile. This technique does not require the retrieval of a water vapor profile before an ozone profile can be retrieved and thus saves computational time.

If computational time is not a concern or if the ozone peak is the particular area of interest then the best retrieval method is the one which uses the retrieved water vapor profile as the *a priori*. This method should also be used if the retrieved profiles deviate greatly from the mean climatological *a priori* profile (this can be shown by a comparison of figure 5.7 and figure 5.8). Because it is a better method when the profile deviation is great, this is the best retrieval method to use in general when the statistical variation of the profiles is not known.

6.6 Rodgers' Error Analysis and RMSE

Rodgers' error analysis provides a more accurate error estimate. It includes the covariances between adjacent altitudes in the calculation of the level-to-level errors. This is more realistic since the emission spectrum observed at a given altitude includes the influence of adjacent emission volumes because of finite antenna beamwidth.

To find the RMSE error, all the ozone retrievals must be done. At 22 minutes per retrieval, when run on a DEC-Alpha machine, a large data set can take an extremely long time to compute. Rodgers' error analysis can take much less time especially if the variability of the constituent in question is well known, since the S_b matrix can then be created without doing any retrievals. The D_b matrix still requires 22 retrievals, but the resultant matrices can be manipulated in most math programs.

In a "real world" retrieval problem, the Rodgers' error for the companion gas problem can be calculated before any ozone profiles are retrieved. The D_b matrix is calculated using the *a priori* profile which, by definition, is known before the retrieval process begins. The S_b matrix can be calculated by using data found from other experiments dealing with the retrieval of ozone and water vapor profiles.

The RMSE **cannot** be computed in a "real world" situation because the true profiles are not known. Therefore, a different method must be used to investigate resulting errors. It has been shown that Rodgers' error analysis is a valid technique to use. Although the numerical values of the error found using RMSE and Rodgers' may differ, the shapes of the error traces are very similar. Therefore an assessment of the error induced in a retrieval using different model parameters is possible.

APPENDIX A

Forward Model

A.1 Introduction

The forward model is a radiative transfer model which mathematically represents the underlying physical basis of the measured spectrum. Included in the model are several factors: a limb-scanning quadrature scheme; the image band contribution (see section 2.4); atmospheric refraction and other factors which may effect the measured spectrum. The main part of the forward model however is a microwave radiative transfer equation. Note that the "limb-scanning quadrature scheme" is just the continuous radiative transfer equation in descrete form.

A.2 Microwave Radiative Transfer Equation

The microwave radiative transfer equation is based on Schwarzchild's equation. This equation expresses the relationship between the radiation absorbed (removed) and emitted (added) as a radiation field passes through a finite volume of gas. Scattering is ignored because it is negligible in the microwave portion of the electromagnetic spectrum in the upper atmosphere.

Schwarzchild's equation can be expressed as:

$$\frac{\partial I(v,s)}{\partial s} = \alpha(v,s) \bullet \left[J(v,s) - I(v,s) \right] \qquad [A.1]$$

where s represents the distance measured along the radiation path through the volume. $I(v,s)$ is the monochromatic radiance within the volume. $J(v,s)$ is the source function for

monochromatic radiance as defined by the Planck function for blackbody emission (equation A.2). $\alpha(\nu,s)$ is the absorption coefficient and $(\partial I/\partial s)$ is the incremental change in the beam intensity due to emission and absorption as it travels through the volume.

The source function (**J**) can be represented by the Planck function for blackbody emission if local thermodynamic equilibrium is assumed:

$$J(\nu,s) = \frac{2h\nu^3}{c^2} \bullet \left[\exp\left(\frac{h\nu}{kT(s)}\right) - 1 \right]^{-1} \qquad \text{[A.2]}$$

In the microwave regime, we can assume **hν/kT<<1**, so equation A.2 can be rewritten as:

$$J(\nu,s) = T(s) \bullet \left(\frac{2k\nu^2}{c^2} \right) \qquad \text{[A.3]}$$

which is the Rayleigh-Jeans limit of the plank function. **T(s)** is the ambient temperature (in Kelvin) at position **s** within the volume, **k** is Boltzmann's constant, and **c** is the speed of light.

Holding frequency ν constant and integrating equation A.1 between points s_a and s_b along the transmission path, and expressing the value in terms of brightness temperature results in the operational form of the microwave radiative transfer equation for a non-scattering medium:

$$T_b(\nu, s_b) = T_b(\nu, s_a) \bullet \exp\left[-\int_{s_a}^{s_b} \alpha(\nu, s)\delta s\right] +$$

$$\int_{s_a}^{s_b} T(s)\,\alpha(\nu, s)\exp\left[-\int_{s}^{s_b} \alpha(\nu, s')\delta s'\right]\delta s \qquad \text{[A.4]}$$

Here T_b is the brightness temperature and all the other variables are defined above

[Godizen, 1995].

APPENDIX B

Inverse Model

B.1 Introduction

This appendix will discuss only the final form of the MAS operational algorithm which uses a multivariate, non-linear maximum likelihood solution. For a derivation of this equation the reader is referred to Goldizen, 1995.

B.2 MAS Operational Algorithm

The MAS operational algorithm is an iterative procedure which converges to the maximum likelihood solution.

$$(X)_{(i+1)} = X_a + \left[S_a^{-1} + \left(K^T \right)_i S_y^{-1} (K)_i \right]^{-1} \bullet \left(K^T \right)_i S_y^{-1} \left[y - (f)_i - (K)_i \left(X_a - (X)_i \right) \right]$$

[B.1]

Here **f** is the vector output limb-scanning radiative transfer model discussed in Appendix A. Each iteration assigns to the current estimate of the solution vector $(X)_i$ a synthetic measurement vector $(f)_i = f\ [(X)_i] = (y)_i$. Then $(y)_i$ is compared to the *a priori* synthetic measurement spectra $(f\ [(X_a)] = (y_a))$. When $(y)_i$ is within a predefined error limit of (y_a), then the associated solution vector $((X)_i)$ is considered the correct retrieved profile and the model ends its iterations.

The vector $(X)_i$ consists of 24 elements: the first 22 elements are current estimates of the volume mixing ratio values at 22 altitudes; the 23rd element is the estimated

sideband ratio (**R**); and the final element is the estimated angular offset ($\delta\theta$). $\mathbf{X_a}$ is an *a priori* solution vector which is used as an initial guess.

The measurement vector (**y**) represents the association of 20 measurement spectra of 46 brightness temperatures each for a total of 920 elements. Each element is a brightness temperature at a specific tangent height and for a specific channel.

$\mathbf{K} = \dfrac{\partial \mathbf{y_i}}{\partial \mathbf{X_i}}$ is the kernel matrix. This matrix is calculated using a finite-differencing technique in which the vector $(\mathbf{X})_i$ is perturbed element by element and the change in the spectrum $(\mathbf{y})_i$ is calculated (similar to the perturbation matrix $(\mathbf{D_b})$ described in section 3.3 and 4.6).

$\mathbf{S_y}$ and $\mathbf{S_a}$ are both covariance matrices. $\mathbf{S_y}$ is the measurement error covariance matrix of the MAS. Since no cross-correlations are assumed $\mathbf{S_y}$ is a diagonal matrix with diagonal elements (variances) determined through careful analysis of the measurement "noise" over many spectra. Since **y** (the measurement vector) is a 920 element vector, $\mathbf{S_y}$ is a 920x920 vector with off-diagonal values of 0.

$\mathbf{S_a}$ is the *a priori* covariance matrix. This matrix does allow for cross-correlation between VMR values at different atmospheric levels and therefore has off-diagonal values which can be nonzero [Goldizen, 1995].

APPENDIX C

Scale Height Profiler Program


```
c  program profiler

     real*4 alt(201), VMR(201), He, Hs, Ae, As, smoothvmr(201,5)
     real*4  reso(1), maxvmr, minvmr
     character datafile*12, output*11
     integer choose
     numres=1

c  This section allows the user to decide whether to profile the data from
c  the water data set or from the ozone data set

     write(*,*) ''
     write(*,*) 'Enter the name of ehr datafile you wish to read.'
     write(*,*) '(include filespec ex: water.dat)'
     read(*,1) datafile
   1 format (A)
     write(*,*) ''
     write(*,*) 'Enter -1- if you are producing a water vapor profile.'
     write(*,*) 'Enter -2- if you want to produce an ozone profile.'
     read(*,*) choose
     write(*,*) ''
     write(*,*) 'Enter the total number of lines of data in that file'
     read (*,*) n

c  Opening and reading from the selected file.

     open(unit=1,file=datafile,status='old')
     do count=1,n
       read(1,10)output,Ae,He,maxvmr,As,Hs,minvmr,reso(1)
  10   format(A,7(1x,f6.4))

c  Here is where the initial profile is created using the scale height
c  equation.

     pi=3.1415927
     do i=1,201
       alt(i)=(i-1)*0.5000000

       vmr(i)=Ae*exp(-abs(alt(i)-maxvmr)/He)+
   $        As*exp(-abs(alt(i)-minvmr)/Hs)
```

```fortran
c       vmr(i)=Ae*sin(alt(i)*2*pi/He)*(1+As/100.0000*sin(alt(i)*2*pi/Hs))
        end do


c This is where the lower 45 km of the aprior water vapor profile is
c figured into any calculated water vapour profile

        if (choose .eq. 1) then
          do i=1,43
            vmr(i)=vmr(i)+2*exp(abs(alt(i)-16)/10)
          end do
          do i=43,90
            vmr(i)=vmr(i)+3*exp(-abs(alt(i)-30)/45)
          end do
        end if


c This section is where the raw profile is smoothed using the resolution of
c the intrument defined by the user.

        do k=1,numres
          num1=reso(k)+1
          num2=201-num1
          do i=1,num1-1
            smoothvmr(i,k)=(vmr(i)+vmr(i+1)+vmr(i+2))/3
          enddo
          do i=num1,num2
            smoothvmr(i,k)=0.000000
            do j=i-reso(k),i+reso(k)
              smoothvmr(i,k)=smoothvmr(i,k)+vmr(j)
            enddo
            smoothvmr(i,k)=smoothvmr(i,k)/(2*reso(k)+1)
          enddo
          do i=num2+1,201
            smoothvmr(i,k)=(vmr(i)+vmr(i-1)+vmr(i-2))/3
          enddo
        enddo


c smoothing of the lower 40km of water vapour profiles
        if (choose .eq. 1) then
        do k=1,numres
          num1=10+1
            num2=80-num1
            do i=1,num1-1
              smoothvmr(i,k)=(vmr(i)+vmr(i+1)+vmr(i+2))/3
            end do
            do i=num1,num2
```

```fortran
          smoothvmr(i,k)=0.000000
        do j=i-10,i+10
           smoothvmr(i,k)=smoothvmr(i,k)+vmr(j)
        end do
        smoothvmr(i,k)=smoothvmr(i,k)/(2*10+1)
       end do
      do i=num2+1,80
         smoothvmr(i,k)=(vmr(i)+vmr(i-1)+vmr(i-2))/3
       end do
    end do
   end if

c  Creating and writing to the output file.

    open(unit=5,file=output,status='new')
     write (5,*) ' '
     write (5,*) ' '
     write (5,*) ' '
     write (5,*) '201   0    0'
     do i=1,201
        write(5,*) alt(i), (smoothvmr(i,k), k=1,numres), vmr(i)
     end do
    close(5)

   end do

   close(1)

   end
```

APPENDIX D

Deviation Profiler Program

```
c    PROFILER USING THE WATER A PRIORI DATA

     Real alt(59),ppmv(59),pekalt,A,gasdev
     Real z, newvmr(59)
     Integer seed

     write(*,*) 'Enter the seed for the random number generator'
     write(*,*) '(must be an integer)'
     read(*,*) seed
c  reading in the apriori file
     open (unit=1, file='water.apr', status='old')
       do i=1,4
         read(1,*)
       end do
       do i=1,59
         read(1,*)alt(i),ppmv(i)
       end do
     close(1)


c  Searching for the peak values
     do i=2,59
       if (ppmv(i) .GT. ppmv(i-1)) then
         pekalt=alt(i)
       end if
     end do



c  Creating the random number file
     open (unit=3, file='rannum.h2o', status='new')
       write(3,*) seed
       do k=1,50


c  Here we call the random number function and add it to the
c  apriori water profile.
       A=gasdev(seed)*0.30
       z=gasdev(seed)*10.00
         do i=1,59
           newvmr(i)=(1+(A*cos(pekalt-z)))*ppmv(i)
         end do
```

```
c   Creating the output files
        open (unit=2, file='water.vmr', status='new')
          do i=1,4
              write(2,*)' '
          end do
          write(2,*) '59              0'
          do i=1,59
            write(2,*) alt(i),newvmr(i)
          end do
        close(2)
        write(3,*) A/0.15,z/5.00
      end do
    close(3)

    END


************************************************************

c   Guassian random number generator

    FUNCTION gasdev(idum)
    Integer idum
    Real gasdev

    Integer iset
    Real fac,gset,rsq,v1,v2,ran1
    Save iset,gset
    Data iset/0/
    if (iset .eq. 0) then
  1   v1=2.0*ran(idum)-1.0
      v2=2.0*ran(idum)-1.0
      rsq=v1**2+v2**2
      if (rsq .gt. 1.0 .or. rsq .eq. 0) goto 1
      fac=sqrt(-2.0*log(rsq)/rsq)
      gset=v1*fac
      gasdev=v2*fac
      iset=1
    else
      gasdev=gset
      iset=0
    end if
    return
    END
```

BIBLIOGRAPHY

Bevilacqua, R.M., J.J. Olivero, P.R. Schwartz, C.J. Gibbins, J.M. Bologna, and D.J. Thacker, 1983: An Observational Study of Water Vapor in the Mid-Latitude Mesosphere Using Ground-based Microwave Techniques, *J. Geophys. Res.*, V. 88, NO. C13, 8523-8534.

Bevilacqua, R.M., D.F. Strogel, M.E. Summers, J.J. Olivero, and M. Allen, 1990: The Seasonal Variation of Water Vapor and Ozone in the Upper Mesophere: Implications for Vertical Transport and Ozone Photochemistry, *J. Geophys. Res.*, V. 95, NO. D1, 883-893.

Chiou, E.W., M.P. McCormick, L.R. McMaster, W.P. Chu, J.C. Larsen, D. Rind, and S. Oltmans, 1993: Intercomparision of Stratospheric Water Vapor Observed by Satellite Experiments: Stratospheric Aerosol and Gas Experiment II Versus Limb Infrared Monitor of the Stratosphere and Atmospheric Trace Molecule Spectroscopy, *J. Geophys. Res.*, V. 98, NO. D3, 4875-4887.

Connor, B.J., A.J. Parrish, and J.J. Tsou, 1991: Detection of Stratospheric Ozone Trends by Ground-Based Microwave Observations, *SPIE Remote Sens. Atmos. Chem.*, V. 1491, 218-230.

Goldizen, D.T., 1995: Characterization and Error Analysis of Millimeter-wave Atmospheric Sounder (MAS) Water Vapor and Ozone Retrievals, Unpublished.

Gunson, M.R., C.B. Farmer, R.H. Norton, R. Zander, C.P. Rinsland, J.H. Shaw, and B.C. Gao, 1990: Measurements of CH_4, N_2O, CO, H_2O, and O_3 in the Middle Atmosphere by the Atmospheric Trace Molecule Spectroscopy Expirement on Spacelab3, *J. Geophys. Res.*, V. 95, NO. D9, 13,867-13,882.

McCormick, M.P., E.W. Chiou, L.R. McMaster, W.P. Chu, J.C. Larsen, D. Rind, and S. Oltmans, 1993: Annual Variations of Water Vapor in the Stratosphere and Upper Troposphere Observed by the Stratospheric Aerosol and Gas Experiment II, *J. Geophys. Res.*, V. 98, NO. D3, 4867-4874.

Press, W.H., Flannery, B.P., Teukolsky, S.A., Vetterling, W.T., 1993: *Numerical Recipies: The Art of Scientific Computing*, Cambridge University Press, New York, NY.

Rodgers, C.D., 1990: Characterization and Error Analysis of Profiles Retrieved from Remote Sounding Measurements, *J. Geophys. Res.*, V. 95, NO. D5, 5587-5595.

VITA

Larry L. Johnson ▮▮▮▮▮▮▮▮▮▮▮▮▮▮▮▮▮▮▮▮n. He lived of the first 17 years of his life in Dallas, Oregon, a small logging town in the Willamette Valley. After graduating from Dallas High School in 1986, Larry attended the University of Washington where he received a Bachelor of Arts degree in Mathematics in June of 1990. That same month he was commissioned a Second Lieutenant in the United States Air Force.

His first Air Force assignment was at Pennsylvania State University for the Basic Meteorology Program where he earned his Bachelor of Science degree in Meteorology. From there he was assigned to March Air Force Base, California where he spent two years as a Wing Weather Officer. In May 1994 he was accepted to the Air Force Institute of Technology. On ▮▮▮▮▮ ▮▮▮▮▮ he married Stacey L. Mason in Spokane, Washington.

REPORT DOCUMENTATION PAGE

1. AGENCY USE ONLY (Leave blank)	2. REPORT DATE December 1995	3. REPORT TYPE AND DATES COVERED Master's Thesis

4. TITLE AND SUBTITLE
COMPARISON OF METHODS FOR ESTIMATING RMS ERROR FOR A SPECIFIC RETRIEVAL ERROR FOR A LIMB-SCANNING MICROWAVE RADIOMETER-SPECTROMETER

5. FUNDING NUMBERS

6. AUTHOR(S)

Larry Johnson, Captain, USAF

7. PERFORMING ORGANIZATION NAME(S) AND ADDRESS(ES)

Air Force Institute of Technology,
WPAFB OH 45433-6583

8. PERFORMING ORGANIZATION REPORT NUMBER

AFIT/GAP/ENP/95D-10

9. SPONSORING / MONITORING AGENCY NAME(S) AND ADDRESS(ES)

Dr. Richard Bevilacqua
Space Science Division
Naval research Lab
4555 Overlook Ave SW
Washington DC 20375-5320

10. SPONSORING / MONITORING AGENCY REPORT NUMBER

11. SUPPLEMENTARY NOTES

12a. DISTRIBUTION / AVAILABILITY STATEMENT

Approved for public release; distribution unlimited

12b. DISTRIBUTION CODE

13. ABSTRACT (Maximum 200 words)

The Millimeter-wave Atmospheric Sounder's operational retrieval algorithm uses an ozone measurement spectrum to retrieve the height dependent vertical ozone concentration profile, but requires a water vapor profile in order to remove the influence of the water vapor spectrum from the ozone spectrum. Currently, the MAS Science Team provides the retrieved water vapor profile as the input to the ozone retrieval algorithm. Our simulation study investigates if this technique results in a smaller error than one in which a single, fixed climatological-mean water vapor profile is employed for all the ozone retrievals.

In answering this question, two error analysis approaches are compared: a simulation study involving 100 synthetic ozone spectra for which an ensemble RMS error between true and retrieved ozone values is calculated, versus a single, elegant, but mathematically-complicated calculation of the associated error covariance matrix as suggested by C. D. Rodgers [1990].

14. SUBJECT TERMS
Ozone, water vapor, Millimeter-wave Atmospheric Sounder, MAS, RMSE spectra, profile, Rodgers' Error Analysis, companion gas, angular offset sideband ratio, forward model, inverse model, a priori profile

15. NUMBER OF PAGES
78

16. PRICE CODE

17. SECURITY CLASSIFICATION OF REPORT Unclassified	18. SECURITY CLASSIFICATION OF THIS PAGE Unclassified	19. SECURITY CLASSIFICATION OF ABSTRACT Unclassified	20. LIMITATION OF ABSTRACT UL